

---

## Hybrid Propulsion for Air Force Applications Study

Kevin E. Mahaffy  
George C. Harting  
Ronald Bates

Phillips Laboratory  
Propulsion Directorate (AFMC)  
Edwards Air Force Base CA 93524-7048

Ray Walsh  
Craig Hansen

W.J. Schafer & Associates  
Calabasas CA 91302

May 1996

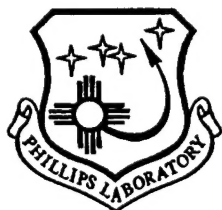
DTIC QUALITY INSPECTED 4

Final Report

---

APPROVED FOR PUBLIC RELEASE; DISTRIBUTION UNLIMITED.

---

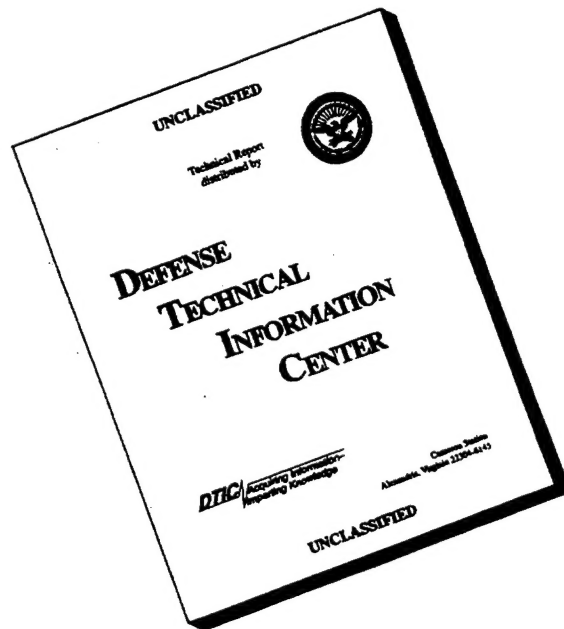


**PHILLIPS LABORATORY**  
**Propulsion Directorate**  
**AIR FORCE MATERIEL COMMAND**  
**EDWARDS AIR FORCE BASE CA 93524-7048**

19960821 011

---

# DISCLAIMER NOTICE



**THIS DOCUMENT IS BEST QUALITY AVAILABLE. THE COPY FURNISHED TO DTIC CONTAINED A SIGNIFICANT NUMBER OF PAGES WHICH DO NOT REPRODUCE LEGIBLY.**

## NOTICE

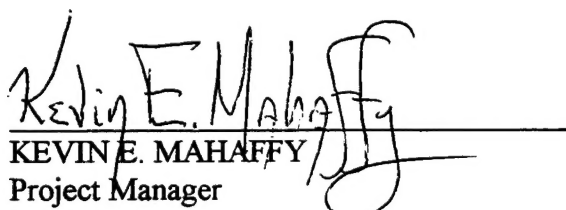
When U.S. Government drawings, specifications, or other data are used for any purpose other than a definitely related Government procurement operation, the fact that the Government may have formulated, furnished, or in any way supplied the said drawings, specifications, or other data, is not to be regarded by implication or otherwise, or in any way licensing the holder or any other person or corporation, or conveying any rights or permission to manufacture, use or sell any patented invention that may be related thereto.

## FOREWORD

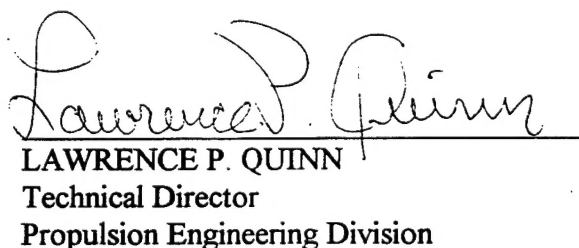
This final technical report was prepared by OL-AC PL/RKEM. The Project Manager at Operating Location AC, Phillips Laboratory, Edwards AFB CA was Mr. Kevin E. Mahaffy.

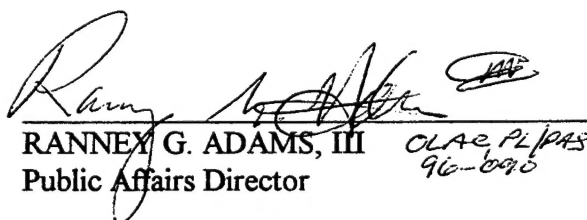
The authors would like to express their sincere gratitude for the help of the following: Mr. Gene Haberman, Lt. Travis Elkins, Mr. James Lynge, Mr. Gregory Price, Dr. Frank Mead, Dr. Jay Levine, the personnel of the Army Missile Command, Naval Air Warfare Center, and the many aerospace companies that were so generous with their time and assistance.

This report has been reviewed and is approved for release and distribution in accordance with the distribution statement on the cover and on the SF Form 298.

  
KEVIN E. MAHAFFY  
Project Manager

  
DREW O. DeGEORGE  
Chief, Motor Branch

  
LAWRENCE P. QUINN  
Technical Director  
Propulsion Engineering Division

  
RANNEX G. ADAMS, III  
Public Affairs Director  
OLAC PL/PAS  
96-090

<b>REPORT DOCUMENTATION PAGE</b>			<b>Form Approved</b> <b>OMB No 0704-0188</b>	
Public reporting burden for this collection of information is estimated to average 1 hour per response, including the time for reviewing instructions searching existing data sources gathering and maintaining the data needed, and completing and reviewing the collection of information. Send comments regarding this burden estimate or any other aspect of this collection of information, including suggestions for reducing this burden to Washington Headquarters Services, Directorate for Information Operations and Reports, 1215 Jefferson Davis Highway, Suite 1204, Arlington, VA 22202-4302, and to the Office of Management and Budget, Paperwork Reduction Project (0740-0188), Washington DC 20503.				
1. AGENCY USE ONLY (LEAVE BLANK)		2. REPORT DATE May 1996		3. REPORT TYPE AND DATES COVERED Final Feb 95-Sep 95
4. TITLE AND SUBTITLE Hybrid Propulsion for Air Force Applications Study			5. FUNDING NUMBERS C: PE: 62601F PR: 1011 TA: CA05	
6. AUTHOR(S) Kevin E. Mahaffy, George C. Harting and Ronald Bates Ray Walsh and Craig Hansen (W.J. Schafer and Associates)				
7. PERFORMING ORGANIZATION NAME(S) AND ADDRESS(ES) Phillips Laboratory (AFMC) OL-AC PL/RKEM 4 Draco Drive Edwards AFB CA 93524-7160			8. PERFORMING ORGANIZATION REPORT NUMBER PL-TR-96-3018	
9. SPONSORING/MONITORING AGENCY NAME(S) AND ADDRESS(ES)			10. SPONSORING/MONITORING AGENCY REPORT NUMBER	
11. SUPPLEMENTARY NOTES COSATI CODE(S): 210801; 160401				
12a. DISTRIBUTION/AVAILABILITY STATEMENT Approved for public release; distribution is unlimited			12b. DISTRIBUTION CODE	
13. ABSTRACT (MAXIMUM 200 WORDS) The Hybrid Propulsion for Air Force Applications Study was performed by the Air Force Phillips Laboratory at Edwards Air Force Base, California. The hybrid propulsion study's four main objectives were 1) to conduct a survey of the current state-of-the-art technology in hybrid propulsion, 2) to determine if there is a payoff for using hybrid propulsion in Air Force missions, 3) to make recommendations as to whether or not hybrid propulsion should be pursued by Phillips Laboratory, and 4) if hybrid propulsion is to be pursued, produce a technology development plan. An industry survey of current state-of-the-art technology in hybrid propulsion identified several advantages and disadvantages associated with hybrid propulsion. Identified areas of concern were combustion efficiency, fuel regression rate, and mixture ratio shifts. The identified Air Force application was the use of a hybrid propulsion system in an air-to-air missile. Volume-limited designs were produced that showed that hybrid propulsion offers good potential for an air-to-air missile that can meet insensitive munitions requirements as well as provide improved energy management. A flight engagement analysis was performed to establish the mission advantage supplied by the hybrid systems formulated in the design task.				
14. SUBJECT TERMS hybrid rocket engines; air-to-air missile; fuel rich gas generator; rocket; propulsion; energy management; oxidizer; expulsion system; injector; insensitive munitions; environmentally clean; grain design; ballistics; specific impulse; fuel; configuration; volumetric analysis; exhaust plumes; low cost air launched; high energy propellants			15. NUMBER OF PAGES 69	
			16. PRICE CODE	
17. SECURITY CLASSIFICATION OF REPORT Unclassified	18. SECURITY CLASSIFICATION OF THIS PAGE Unclassified	19. SECURITY CLASSIFICATION OF ABSTRACT Unclassified	20. LIMITATION OF ABSTRACT SAR	



## TABLE OF CONTENTS

1.0	Executive Summary .....	1
2.0	Hybrid Propulsion System Description .....	3
2.1	Classical Inert Systems .....	6
2.2	Gas Generator Systems .....	8
2.2.1	Aft-Injected Gas Generator Cycle .....	8
2.2.2	Forward-Injected Gas Generator Cycle .....	9
3.0	Technology Application to Air Force Missions .....	12
4.0	Tactical Study .....	13
4.1	Program Plan .....	13
4.2	Tactical Missile Hybrid Technology System Study .....	13
4.3	Design Configurations .....	18
4.3.1	Design Considerations .....	18
4.3.2	FIGG Cycle Designs (Standard Length) .....	20
4.3.3	Staged Combustion Cycle Designs (Standard Length) .....	35
4.3.4	FIGG Cycle Designs (+15% Length) .....	49
4.3.5	Staged Combustion Cycle Designs (+15% Length) .....	52
4.4	Engagement Analyses .....	55
4.4.1	Hybrid Motor Performance Characteristics .....	55
4.4.2	Candidate Missile Flight Performance .....	55
4.4.3	Engagement Analysis Summary .....	59
4.5	Tactical System Summary .....	60
5.0	Tactical Technology Development Elements .....	61
5.1	Cycle Common Elements .....	61
5.2	Cycle Unique Elements .....	61
6.0	Summary and Conclusions .....	62

## LIST OF FIGURES

Figure 1	Schematic of a Classical Inert Hybrid Booster .....	4
Figure 2	Some Possible Cycle Selections.....	5
Figure 3	Simplified Heat Transfer Processes in Solid-Gas Diffusion Flame .....	6
Figure 4	Impact of Increasing Regression Rate Correlation Coefficient on Grain Cross Section .....	7
Figure 5	Schematic of Aft-Injected Gas Generator Concept .....	9
Figure 6	Schematic Drawing of the Forward-Injected Gas Generator Concept.....	10
Figure 7	Multiple Flame Zones that May Exist Near Gas Generator Burning Surface .....	10
Figure 8	Classical Cycle Shutdown and Throttling .....	17
Figure 9	Gas Generator Cycle Shutdown and Throttling .....	17
Figure 10	FIGG Cycle Shutdown and Throttling .....	18
Figure 11	Standard Length FIGG Hybrid Motor Pressurization System .....	23
Figure 12	Standard Length FIGG Hybrid Motor Layout .....	24
Figure 13	Standard Length FIGG Hybrid Motor Oxidizer Tank .....	25
Figure 14	Standard Length FIGG Hybrid Motor Flow Control Valve .....	26
Figure 15	Standard Length FIGG Hybrid Motor Distribution Plate .....	27
Figure 16	Standard Length FIGG Hybrid Motor Injector .....	28
Figure 17	Standard Length FIGG Hybrid Motor Case.....	30
Figure 18	Standard Length FIGG Hybrid Motor Propellant Insulation.....	31
Figure 19	Standard Length FIGG Hybrid Motor Solid Propellant.....	32
Figure 20	Standard Length FIGG Hybrid Motor Nozzle.....	32
Figure 21	Standard Length FIGG Hybrid Motor Nozzle Insulation .....	33
Figure 22	Standard Length FIGG Hybrid Motor Ignition Unit .....	33
Figure 23	Standard Length FIGG Hybrid Motor Missile Configuration.....	35
Figure 24	Standard Length Staged Combustion Hybrid Motor Pressurization System .....	38
Figure 25	Standard Length Staged Combustion Hybrid Motor Layout.....	39
Figure 26	Standard Length Staged Combustion Hybrid Motor Oxidizer Tank .....	40
Figure 27	Standard Length Staged Combustion Hybrid Motor Flow Control Valve .....	40
Figure 28	Standard Length Staged Combustion Hybrid Motor Distribution Plate .....	41
Figure 29	Standard Length Staged Combustion Hybrid Motor Injector .....	42
Figure 30	Standard Length Staged Combustion Hybrid Motor Motor Case.....	44
Figure 31	Standard Length Staged Combustion Hybrid Motor Propellant Insulation.....	44
Figure 32	Standard Length Staged Combustion Hybrid Motor Propellant .....	45
Figure 33	Standard Length Staged Combustion Hybrid Motor Nozzle.....	45
Figure 34	Standard Length Staged Combustion Hybrid Motor Nozzle Insulation .....	46
Figure 35	Standard Length Staged Combustion Hybrid Motor Ignition Unit .....	47
Figure 36	Standard Length Staged Combustion Hybrid Motor Missile Configuration .....	49
Figure 37	+15% Length FIGG Hybrid Motor Layout .....	51
Figure 38	+15% Length FIGG Hybrid Motor Missile Layout.....	52
Figure 39	+15% Length Staged Combustion Hybrid Motor Layout .....	54
Figure 40	+15% Length Staged Combustion Hybrid Motor Missile Configuration.....	55
Figure 41	Engagement Geometries and Selected Engagements .....	57
Figure 42	Trajectory Shaping and Propulsive Energy Management .....	58
Figure 43	Flight Constraints and Missile Configurations .....	59

## LIST OF TABLES

Table 1	Oxidizers and Fuel Densities.....	14
Table 2	Impulse and Density Impulse for Candidate Tactical Hybrid Systems .....	15
Table 3	Summary of Packaged Total Impulse.....	16
Table 4	Candidate Propellant Operating Points .....	16
Table 5	Performance Results for Candidate Hybrid Rocket Propellants.....	20
Table 6	Materials Used in Construction of Hybrid Rocket Motors .....	21
Table 7	Physical Properties of FIGG Hybrid Rocket Motors .....	22
Table 8	FIGG Hybrid Rocket Motor Performance.....	24
Table 9	Material Properties of Liquid Components of a FIGG HRM.....	29
Table 10	Material Properties for Solid Components of a FIGG HRM.....	34
Table 11	Staged Combustion Hybrid Rocket Performance .....	35
Table 12	Materials Used in the Construction of FIGG and SC HRMs .....	36
Table 13	Comparison of Physical Properties of FIGG and SC HRMs.....	37
Table 14	Comparison of Hybrid Rocket Motor Performance for FIGG and SC HRMs.....	39
Table 15	Material Properties Comparison of Liquid Components of Two HRMs.....	43
Table 16	Material Properties Comparison of Solid Components of Two HRMs .....	48
Table 17	Materials Used in the Construction of FIGG and +15% HRMs .....	49
Table 18	Comparison of Physical Properties of FIGG and +15% HRMs.....	50
Table 19	Comparison of Performance for FIGG and +15% FIGG HRMs.....	51
Table 20	Materials Used in Construction of FIGG, +15% FIGG, SC and +15% SC HRMs.....	52
Table 21	Comparison of Physical Properties of FIGG and SC HRMs.....	53
Table 22	Comparison of Performance for FIGG and SC HRMs.....	54

## Glossary

Abbreviation	Description
A	missile body cross section area
$A_b$	burning surface area
AIGG	aft-injected gas generator
AP	ammonium perchlorate
$A_p$	port area
$A_t$	throat area
a	coefficient in hybrid regression rate correlation
BAMO	3,3-Bis (azidomethyl) oxetane polymer
BMDO	Ballistic Missile Defense Organization
BVR	beyond visual range
BVRM	beyond visual range missile
CA	chord force coefficient
Cd	discharge coefficient
CN	normal force coefficient
CSD	Chemical Systems Division (of United Technologies)
$c^*$	characteristic velocity
EB	electron beam
EDM	electric discharge machining
EPDM	ethylene-propylene-unconjugated diene terpolymer
FIGG	forward-injected gas generator
GAP	glycidl azide polymer
GAP-A	glycidl azide-A polymer
$G_F$	flame zone mass flux
GG	gas generator
GOX	gaseous oxygen
g	gravity
HAN	hydroxylammonium nitrate
HRM	hybrid rocket motor
HTPB	hydroxyl-terminated polybutadiene
$H_2O_2$	hydrogen peroxide
IRFNA	inhibited red fuming nitric acid
ISI	Integrated Systems Incorporated
Isp	specific impulse
L	length
LOX	liquid oxygen
M	Mach number
MR	mixture ratio
NASA	National Aeronautics and Space Administration
$NH_4NO_3$	ammonium nitrate
NTO	nitrogen tetroxide
$N_2O$	nitrous oxide
n	mass flux or pressure exponent in regression rate
O/F	oxidizer to fuel ratio
P	pressure
$P_c$	chamber pressure
$P_e$	exit pressure
$P_{GG}$	gas generator pressure
PL	Phillips Laboratory
PLOX1	Notional Advanced Oxidizer

$\dot{Q}_r$	radiant heat flux
$R_{f-p}$	f-pole range
$R_i$	missile intercept range
$R_L$	missile launching range
ROM	rough order of magnitude
RP	rocket propellant
$r$	radius
SC	staged combustion
SOTA	state of the art
T	temperature
$T_e$	boundary layer external temperature
THF	tetrahydrofuran
$T_s$	surface temperature
$u_e$	boundary layer external velocity
USAF	United States Air Force
WJSA	W. J. Schaefer Associates, Inc.
$\Delta P$	pressure drop
$\Delta P_{inj}$	injector pressure drop
$\Delta T$	temperature difference from flame zone to fuel surface
$\alpha$	angle of attack
$\kappa_g$	gas-phase thermal conductivity
$\rho$	density
$\rho_e$	boundary layer external density
$(\rho v)_s$	surface blowing mass flux
$\sigma_s$	surface radiative emissivity
$\xi$	fluids-to-solid ratio

## 1.0 EXECUTIVE SUMMARY

The Hybrid Propulsion for Air Force Applications Study was performed by the Air Force Phillips Laboratory (PL) at Edwards Air Force Base. The tactical study was accomplished in conjunction with a support contractor, W. J. Schafer Associates, Inc (WJSA). A complementary spacelift booster study was performed in-house with Phillips Laboratory personnel. The performance period extended from mid-February through September 1995. The technical effort was approximately three-quarters of a man-year.

The hybrid propulsion study's four main objectives were to:

1. conduct a survey of the current state-of-the-art technology in hybrid propulsion,
2. determine if there is a payoff for using hybrid propulsion in Air Force missions,
3. make recommendations as to whether or not hybrid propulsion should be pursued by Phillips Laboratory, and
4. if hybrid propulsion is to be pursued, produce a technology development plan.

One conclusion of the survey was that competitive niches for hybrids can exist. It will be mission constraints that determine the suitability of hybrids for any particular application. Hybrid advantages are chiefly qualitative and are more difficult to substantiate (e.g., safety, reliability, throttling, shutdown, environmental impact, cost). Hybrid disadvantages are often quantitative with significant technical basis (e.g., mass fraction, specific impulse (Isp), density impulse, combustion efficiency, mixture ratio shift). However, it was judged that there are no insurmountable obstacles that preclude hybrid development. Hybrid weaknesses in combustion stability and efficiency, burn rates, liquid feed system, injector configuration, and repeatability can be addressed with appropriate development efforts.

The United States Air Force (USAF) tactical community did identify a need for improved performance for air-to-air missiles. In addition, the USAF expressed an interest in positioning itself to satisfy the goals of insensitive munitions for future new missile systems. That goal could preclude the use of advanced high energy solids necessary to eliminate the performance shortfall of current systems. Thus a decision was made at the end of March 1995 to focus this study on the formulation of hybrid motor designs for the tactical missile application.

A solid propellant baseline was used as the basis for scaling inert weights for the hybrid designs. The external envelope was held constant (i.e., all designs were volume constrained). The nominal thrust level for the hybrids was the same as for the solid baseline. Design methodology for the hybrids was consistent with that used in generating the solid baseline. However, optimistic levels of engineering judgment were applied to the new hybrid designs to determine the hybrids' ultimate potential. An example would be the assumption of a 95% energy release efficiency (typical state-of-the-art (SOTA) values are in the range of 87% to 94%). Two motor lengths were evaluated: a standard length (75-in) and a +15% (86-in) length.

Two hybrid combustion cycles were evaluated: a staged combustion or aft-injected gas generator (AIGG), and the forward-injected gas generator (FIGG) cycle. The FIGG cycle is an intriguing combination of the staged combustion cycle and the classical cycle, wherein the benefits of the classical injector and liquid plumbing are combined with the advantages of a gas generator type solid grain.

Propellant combinations were evaluated on an Isp and density impulse basis. Five candidates were down-selected for a preliminary packaging evaluation. On the basis of maximum packaged total impulse, the best propellant combination was used for the detailed layout configuration analyses.

The following are the major conclusions from the tactical design effort: 1) Although hybrid motor mass fractions are slightly lower than the solid, the total impulse delivered by the hybrid is slightly higher than the solid; 2) The FIGG and staged combustion mass fractions are nearly the same (within a few percent); 3) Lightweight and compact oxidizer pressurization and expulsion

components are critical for attaining high mass fractions; 4) Lightweight and compact multiple-use oxidizer control valves are necessary for energy management.

A flight engagement analysis was performed to establish the mission advantage supplied by the hybrid systems formulated in the design task. The OTIS computer code was used to determine the f-pole range for the standard and +15% solid and PLOX1/3,3-bis (azidomethyl) oxetane polymer (BAMO) hybrids. Co-altitude, shoot-up, and shoot-down scenarios were considered. Implementing throttling adds complexity, increases inert weight, and reduces average Isp. For the hybrid, the impulse split between the first and second burn was approximately 60/40. The thrust and impulse for the solid baseline reflects typical characteristics: a boost/sustain thrust profile (with a 1.0/0.5 thrust ratio) and a one-third to two-thirds boost/sustain impulse split.

Results from OTIS indicate that hybrid f-pole gains beyond its impulse advantage may be expected. These higher gains are attributed to a combination of nonlinear impulse sensitivity and energy management. It was observed that optimum second pulse firing delay times varied from 0 to 18 sec. The gains with the hybrids appear to be significant. The flexible energy management that hybrids offer show promise of further gains.

Hybrids can offer significant potential for tactical applications: high performance propellants with the prospect of meeting "insensitive munitions" goals; competitive total impulse capability; and energy management flexibility. Because of the small scale and lower complexity of the tactical application, motor development can be accomplished with compressed schedules and at a reasonable cost. The critical technologies requiring demonstration for the successful implementation of a tactical motor include: 1) gas generator fuel grain formulations and characterization; 2) liquid oxidizer formulations and characterization; 3) liquid oxidizer pressurization and expulsion systems; and 4) a liquid oxidizer injector and feed system.

It was the strong recommendation of the study team that if Air Force propulsion research funding levels permit, hybrid propulsion can be a high payoff technology that should be developed. The team recommended that both forward- and aft-injected gas generator hybrid propulsion be investigated for the tactical mission.

## 2.0 HYBRID PROPULSION SYSTEM DESCRIPTION

The operating principle of a hybrid rocket is based on the utilization of two separated propellants, a liquid and a solid. Thus the features, advantages, and components of a hybrid system are derived from liquid and solid rockets. Figure 1 shows an example of a classical inert hybrid. The distinguishing characteristics of a hybrid propulsion system are the cycles chosen. The combustion cycle options are manifold and can be identified by the following criteria:

1. Solid phase
  - oxidizer
  - fuel
  - gas generator rich in oxidizer or fuel
2. Liquid phase
  - oxidizer
  - fuel
3. Location of injection
  - forward of grain
  - aft of grain
  - combination of both

Figure 2 shows most of the permutations of the above criteria. While hybrid systems containing an oxidizer rich grain were considered, this option has not been accepted because of potential grain safety problems and low performance. The following sections describe what three systems have been considered historically, except for the reverse hybrid concept (an oxidizer rich grain burned with a liquid fuel), which has also been studied and fired in the mid-sixties. This concept was not considered in this study, though extremely useful information can be extracted from the experimental data, such as the possible existence of two flame zones for the forward-injected gas generator concept.



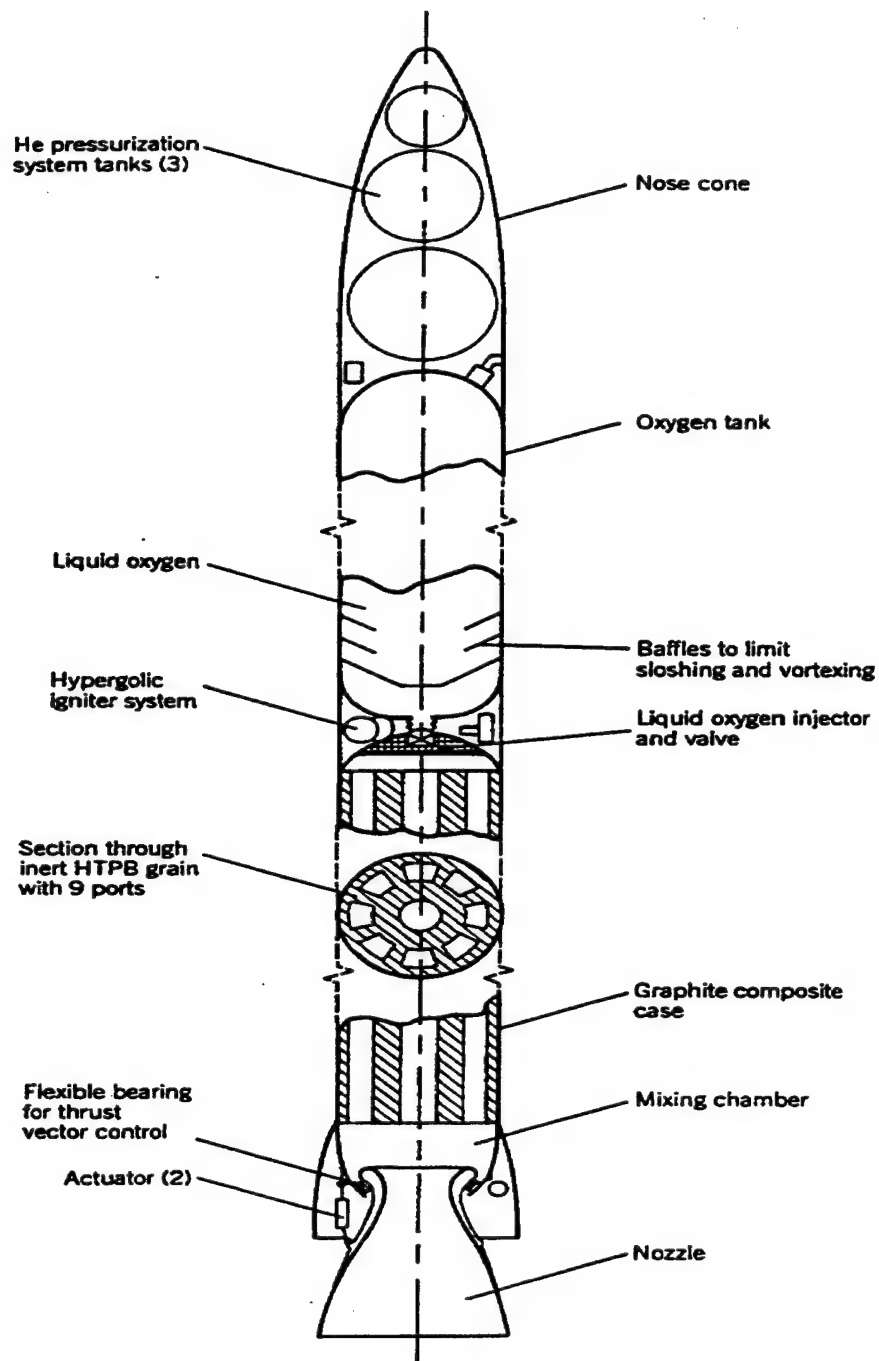


**Figure 1**  
**Schematic of a Classical Inert Hybrid Booster**

Rocket Propulsion Elements, George P. Sutton, Copyright ©1992, John Wiley & Sons, Inc. Reprinted by permission of John Wiley & Sons, Inc.

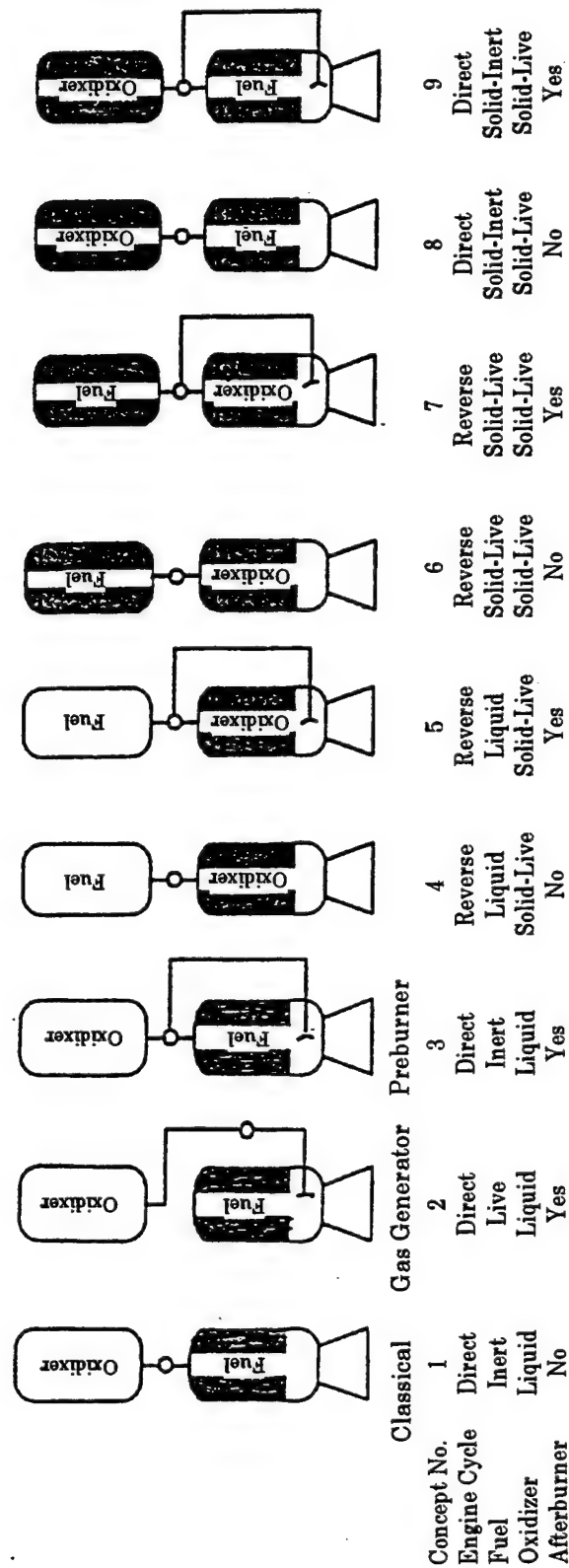


Figure 2  
Some Possible Cycle Selections

Analogous to its operation, the hybrid contains hardware elements from both its solid and liquid rocket relatives. The solid-related major components include: solid grain with its attendant grain design, supports, insulation, and inhibitors (as necessary), solid motor high pressure case, and exhaust nozzle. The liquid-related major components include: oxidizer tank and liquid acquisition system, tank pressurization, feed lines, injector, and control valves (shutoff and/or throttling). If the liquid is pump-fed, then the pump, turbine and turbine drive gas systems are necessary.

## 2.1 Classical Inert Systems

The design of the classical hybrid system considers the use of a solid inert fuel grain and a forward-injected liquid oxidizer, as shown in Figure 1. This option is the design that is currently being supported by NASA in the Hybrid Propulsion Program. The use of an inert grain increases the safety margin of the design when compared to the gas generator cycles. Also, the injector system is expected to be much more simple than liquid engine systems. The difficulties associated with the atomization and mixing of two fluid streams will not be involved since only the oxidizer needs to be injected into the combustion chamber. However, other difficulties that are hybrid unique may form, such as the impingement of atomized oxidizer on the solid fuel grain. Since the grain is inert, heat produced in the diffusion flame zone needs to be transferred back to the fuel surface via convective and diffusive means. Figure 3 shows some of the heat transfer processes involved.

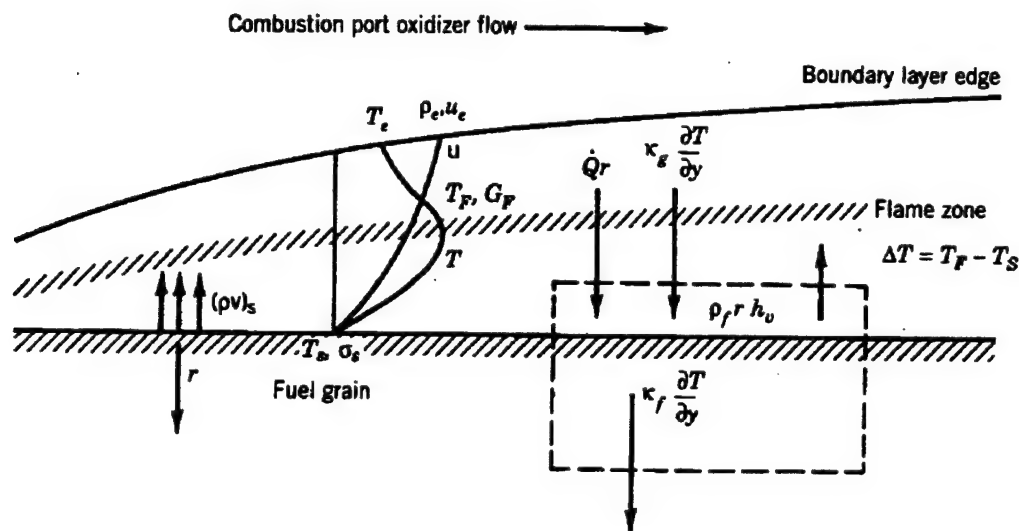


Figure 3

### Simplified Heat Transfer Processes In Solid-Gas Diffusion Flame

Rocket Propulsion Elements, George P. Sutton, Copyright ©1992, John Wiley & Sons, Inc. Reprinted by permission of John Wiley & Sons, Inc.

Within the operating parameters found in a hybrid rocket motor, traditional turbulent heat transfer to the fuel will be dependent on the mass flux level raised to the 0.8 power. The heat transfer dependence on mass flux in turn causes the regression rate to be dependent on mass flux. What implications does flux dependence have on the actual grain design? In summary, the dependence of the regression rate on flux may require some degree of fuel tailoring to maximize performance. The ability of a hybrid to throttle usually entails operation at fuel rich or lean conditions, leading to a lower specific impulse.

Typical regression rates for classical inert systems are about an order of magnitude lower than solid propellant burn rates. For example, typical composite propellants have burn rates that

can range from 0.3 to 0.5 in per sec at 1000 psia while hybrid propellants (liquid oxygen (LOX)/hydroxyl-terminated polybutadiene (HTPB)) have regression rates less than 0.1 in per sec for an oxidizer mass flux of 1.0 lbm/in<sup>2</sup>-sec. The rationale for such low regression rates lies in the fundamental structure of the flame zone and the processes involved in heat transfer. Because the solid grain is composed entirely of fuel, the process of mixing oxidizer and fuel is dependent on the mechanism of diffusion and convection of the oxidizer from the freestream and through the boundary layer. Similarly, the fuel vapors being produced at the grain surface must travel within the boundary layer to the flame zone. The mixing and combustion subsequently take place at a relatively large stand-off distance from the fuel surface. For solid propellant systems, by intimately "pre-mixing" the oxidizer and fuel in the solid grain, the characteristic mixing scales are much smaller. The feedback of heat to the solid grain surface (which translates to regression/burn rate) depends on flame stand-off distances, which is greater for classical inert hybrids than for solid propellant motors.

The impact of a flux-dependent, low-regression rate fuel is reflected in the fuel grain design. To meet fuel mass flow requirements, the regression rate sets a certain burning surface area requirement. The flux dependence of regression rate, in turn, determines the port area requirements for a given mass flow rate. These two factors greatly shape the solid fuel grain design. Several obvious and not so obvious results can be summarized in the following:

1. High regression rates lead to higher volume loading
2. Volume loading is limited by port mass flux (e.g., limitations caused by stability issues)
3. High regression rates reduce the number of ports
4. Lower number of ports reduces the amount of unusable fuel (sliver)
5. Lower number of ports reduces the expected shift in oxidizer-to-fuel (O/F) ratio

Some of the results of the analysis can be seen in Figure 4, which shows several grain cross sections and their regression rates relative to the slowest burning fuel.

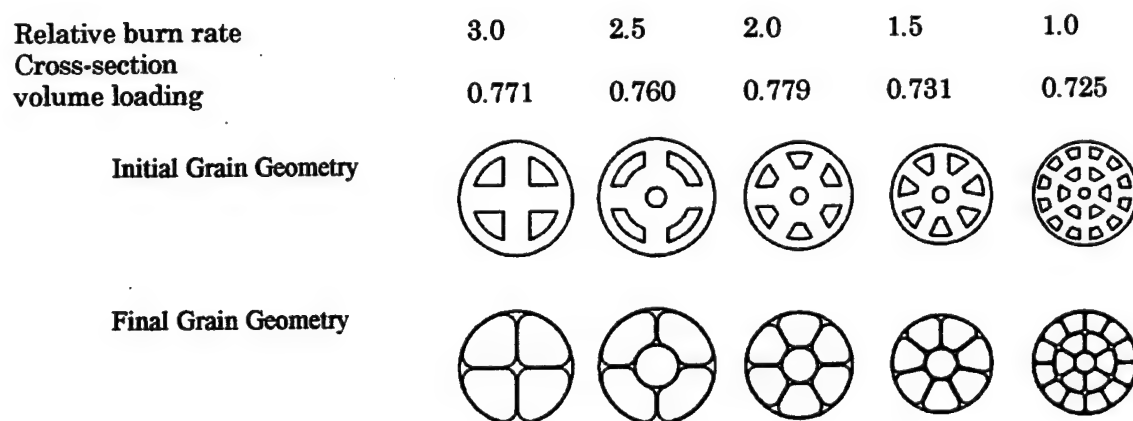


**Figure 4**  
**Impact of Increasing Regression Rate Correlation Coefficient**  
**on Grain Cross Section**

Another important aspect in the classical inert cycle is the ability of the gaseous fuel and oxidizer to mix and combust. Often, the combustion within the port is incomplete and an aft mixing chamber is needed to provide a sufficient amount of residence time for the fuel to completely combust.

## 2.2 Gas Generator Systems

Concern over the regression rate that is typical of inert fuels leads to the consideration of solid propellant gas generator-based hybrid cycles. Often using a fuel-rich solid propellant, the gas generator hybrid cycles try to take advantage of the higher regression rates and pressure dependence of solid propellants. If the cycle is solely pressure dependent, the grain design can draw from the extensive experience in solid propellants. The decoupling of the regression rate from port mass flux simplifies the grain design caused by reduced dependence on the port area. Many of the designs in the sixties used fuel-rich gas generator hybrids which operated very similarly to fluid controlled solid propellant motors, but at much higher fluids/solids ratios. Higher regression rates would minimize the required number of ports, the optimum being a one-port design. This, in turn, leads to less sliver and better possible volume loading.

The ability to program into the grain some of the expected throttling requirements that the booster must produce would increase performance by maintaining optimum oxidizer-to-fuel ratios. The liquid system would be used to make fine adjustments as payload requirements dictated, as well as maintain launch vehicle stability during flight.

As always, everything comes with a price. The often-touted inertness of the solid fuel grain would be lost. The degree to which the safety margin of the fuel grain is reduced depends on the classification of the solid propellant. Usually, the low pressure deflagration limit of fuel-rich, solid-propellant gas generators are relatively high compared to commonly employed solid propellants used in boosters. Gas generator systems also need high pressure exponent burn rates to have greater control over motor pressure with the liquid injection system. Since chamber pressure is proportional to mass flow rate, to have a one-to-one correspondence between oxidizer mass flow rate change and solid fuel regression rate, a unity exponent would be required. The additional requirement of fluid reduces the sensitivity of the solid propellant to perturbations in burn surface and nozzle areas. This is shown in the following equation:

$$\frac{dP}{P} = \frac{1}{(1+\xi-n)} \cdot \left[ \frac{dA_b}{A_b} - (1-\xi) \frac{dA_t}{A_t} \right] \quad (1)$$

The presence of  $\xi$ , fluids-to-solid ratio, in the denominator in the first term on the right-hand side reduces the pressure sensitivity because of nozzle throat or burn surface area perturbations. The required presence of fluid for proper operation yields a lower effective propellant burn rate exponent.

**2.2.1 Aft-Injected Gas Generator Cycle.** The aft-injected gas generator cycle concept contains a fuel-rich, solid propellant gas generator grain whose products are fed into an aft section in which the liquid oxidizer is injected. Furthermore, several aft-injected designs for tactical systems were demonstrated in the late-sixties. Figure 5 shows the location of major components of an aft-injected hybrid gas generator.

One problem of the classical inert hybrid was the poor level of mixing within the combustion port of a hybrid, especially for very large diameter motors. The aft-injected concept tries to address this problem by utilizing the controlled mixing environment of a gas-liquid injector design. Second, the expected lower volume loading of the classical inert grain also contributed to the consideration of an aft-injected gas generator cycle. Since a gas generator system is a solid propellant, the higher volume loading of a solid propellant can be used. Furthermore, since half of the mass flow required for the propulsion system comes from the gas generator grains, even higher volume loadings may be possible since the minimum port area to avoid erosive burning effects would be smaller. The minimum port area also would be restricted by the nozzle throat area size. Finally, typical fuel-rich gas generator grains have a low level of solids loading, allowing higher web thickness because of the improved mechanical properties.

Several difficulties also need to be addressed in the selection of an aft-injected system. One question is whether an aft-injected system could be a competitive design with current technology. In

essence, an aft-injected system is very similar to a liquid rocket engine minus a fuel turbopump. From the inlet of the gas-liquid injector to the exhaust, the aft-injected system would rely heavily on liquid engine technologies and have problems (and benefits) associated with such systems. For example, injector designs may be more complex because of matching between two fluid flows (atomization and mixing). Often, engine instability limits the size of liquid engines without using complicated baffles and multiple chambers. The similarity between the aft-injected hybrid and a liquid engine also allows the hybrid system to draw on the design knowledge of liquid engine design.

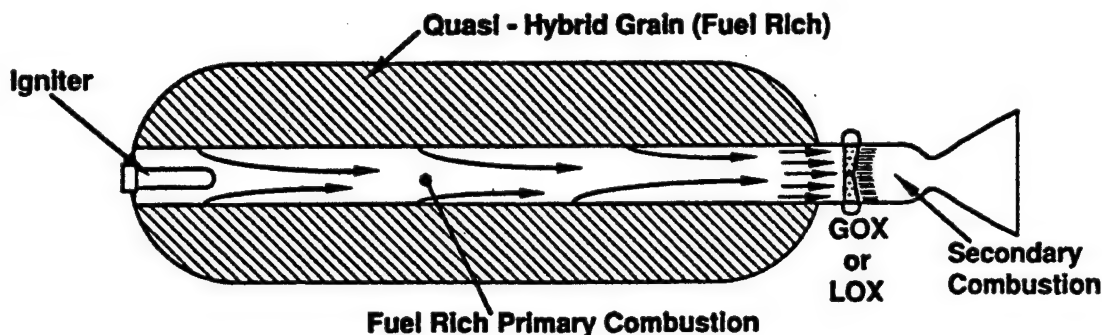


**Figure 5**  
**Schematic of Aft-Injected Gas Generator Concept**

Also, the higher density solid propellant gas generator grain allows for more efficient motor volumes compared to current liquid engines. For example, typical liquid boosters would utilize LOX/RP-1 as propellants. While a hybrid booster would also use LOX as an oxidizer, the solid propellant gas generator grain would have a density about 20 to 40% higher than RP-1. This does not necessarily translate into a volume that is 20 to 40% smaller; therefore, side-by-side comparisons of actual booster designs would have to be made.

Higher density grains may be made by metallizing the fuel, but this could have deleterious effects on the injector. From the standpoint of new engine development, the issues revolving around the aft-injected gas generator cycle probably make it a competitive option if the associated costs of a liquid engine development program are acceptable, i.e., the choice between developing a liquid engine booster and an aft-injected booster is not clear because of the similarities of the two systems. The decision may be narrowed down to four possible reasons: the density of the aft-injected hybrid, the expected benefits of half the feed system, safety concerns of using solid propellants, and the development risk of a new engine technology

**2.2.2 Forward-Injected Gas Generator Cycle.** The forward-injected cycle utilizes a forward-injected oxidizer and a fuel-rich, solid gas generator grain. This design was studied concurrently with the aft-injected gas generator cycles during the research conducted in the late sixties. This concept could be considered an outgrowth of fluid controlled solid propellant research conducted in the same time frame, but at much higher fluid/solid ratios. Figure 6 shows the general design of forward-injected gas generator systems (note the similarity with classical inert systems).

The forward-injected gas generator concept addresses the low volume loadings associated with flux-dependent, low-regression rate inert fuels while maintaining the simplicity of the classical inert system cycle. The regression rate of a flux-controlled fuel depends on several parameters, one of which is the effective heat of vaporization of the fuel. Utilizing a solid gas generator grain effectively lowers the value of the heat of vaporization by the addition of oxidizers in the fuel grain. Thus the heat transfer requirements from the flame zone to the solid fuel would be reduced,

potentially increasing regression rates, assuming the fuel is controlled by the diffusion flame, flux-controlled mechanism. However, the "mode" at which the solid fuel burns is not necessarily clear. Figure 7 shows a rough picture of the many processes involved during combustion of a fuel-rich, solid gas generator grain with an oxidizer crossflow.

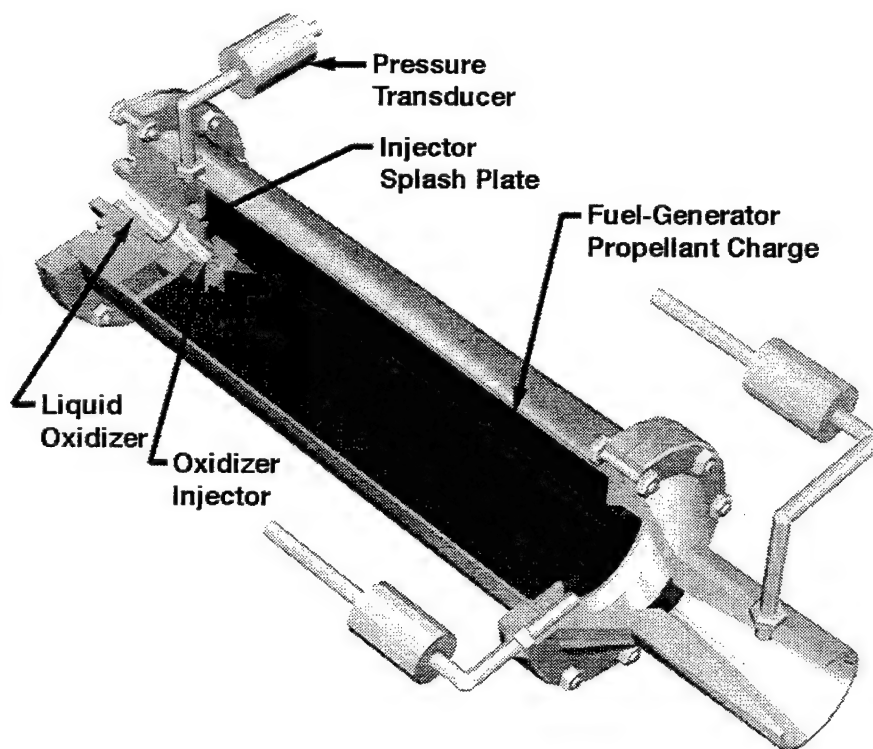


**Figure 6**  
**Schematic Drawing of the Forward-Injected Gas Generator Concept**

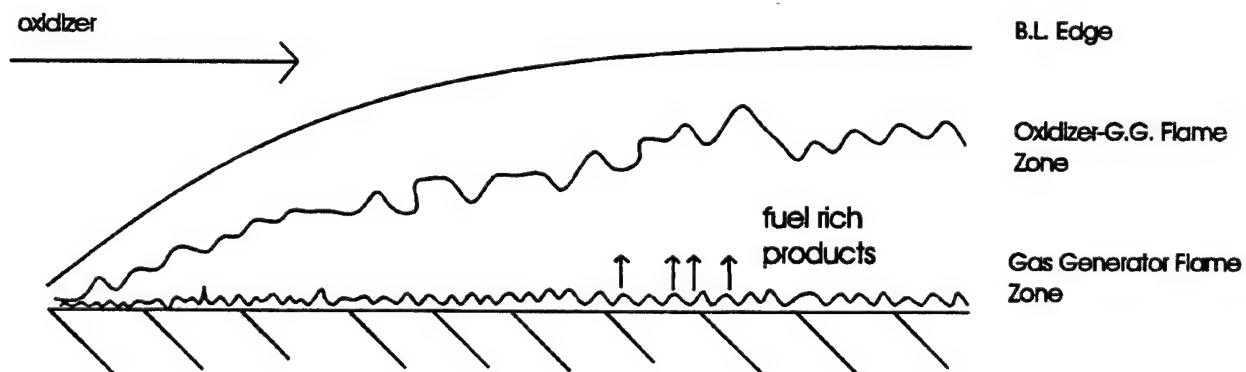


**Figure 7**  
**Multiple Flame Zones That May Exist Near Gas Generator Burning Surface**

The issue that needs to be addressed is the true heat transfer feedback mechanism from the hot gas phase to the solid phase fuel. Much of the early research performed during the late sixties tends to



suggest that solid fuel has a greater pressure dependence as the solid is loaded with higher amounts of oxidizer, which makes sense. However, the ability of the solid gas generator grain to sustain combustion can also be correlated with the oxidizer level within the solid grain, increasing the safety concerns. Finally, the degree to which the solid gas generator grain exhibits a flux-controlled regression rate could also be dependent on the level of port mass flux. Higher levels of flux could increase the turbulence levels within the port, increasing the level of heat transfer attainable from the diffusion flame, i.e., a threshold value of flux changes the heat transfer "mode".

Regardless of the degree to which the solid gas generator fuel exhibits flux and/or pressure dependence, the regression rate is expected to be greater for the forward-injected gas generator than the classical inert fuel system. The higher regression rate could reduce the number of ports needed to meet mass flow requirements while increasing the volume loadings to typical solid propellant motor loading. As with the aft-injected schemes, the mechanical properties of the solid fuel grain may be better because of the decreased solids loadings, therefore allowing higher web fractions. However, the volume loading of the solid fuel grain may be restricted by port flux requirements to avoid erosive burning and nozzle restrictions.

Several other issues can be raised for the forward-injected gas generator cycle. Combustion stability may benefit from the ability of the solid gas generator grain to act as a pilot light or oxidizer preheater. The combustion efficiency of forward-injected systems could be as low as classical inert systems or as high as aft-injected systems. The ability of the oxidizer core flow to mix with the fuel-rich gas generator products depends on turbulence levels within the port. Additional mixing aids, such as trips or aft-mixing chambers, may be necessary. The injector for the forward-injected system should be similar to the classical inert systems, simplifying the design by injecting only one working fluid into the combustion chamber.



### **3.0 TECHNOLOGY APPLICATION TO AIR FORCE MISSIONS**

One goal of this study was to identify an Air Force mission which hybrid technology could satisfy. It was not the intent to formulate a convenient application to justify the technology. To that end, the Space and Tactical Air Force user communities were interrogated for needs in the three generic classes of propulsion systems: booster, upper stage, and tactical. The team (a combined PL/WJSA effort) could not identify booster or upper stage applications for new propulsion systems since payloads on the USAF manifest could be launched with existing vehicles. No hybrid launch vehicle applications were selected.

The USAF tactical community did identify a need for more performance in future air-to-air missiles. They were actively seeking new technology to increase missile performance within existing volume constraints and insensitive munitions goals. Thus a decision was made to focus on a generic air-to-air tactical missile for the balance of the study's design effort since there was a good prospect that hybrids could deliver competitive performance with increased margins of safety.

## 4.0 TACTICAL STUDY

### 4.1 Program Plan

A joint PL/WJSA team surveyed industry and government agencies participating in hybrid rocket technology. After selecting a candidate Air Force hybrid application, WJSA formulated and designed hybrid motors. These new motors were assimilated into missile systems and flown in engagement simulations. Rough order of magnitude (ROM) schedules and cost estimates for the development of the necessary technology to implement the motor designs were generated. The final briefing and final report were prepared. The final briefing was presented at the Phillips Laboratory on August 31, 1995, as part of a combined PL/WJSA briefing.

### 4.2 Tactical Missile Hybrid Technology System Study

The approach was to establish a solid propellant baseline for a generic, air-to-air missile. The performance parameters were representative of current systems. However, exact performance specifications were avoided.

The solid baseline uses HTPB/ammonium perchlorate (AP) solid propellants. The solid baseline inert weights were used as a scaling basis for the hybrid configurations. Because the mission application is volume constrained, the motor envelopes for the solid-to-hybrid comparisons were held constant. The hybrid maximum thrust was made approximately equal to the solid maximum thrust. In addition, the design methodology (e.g., materials, safety factors, etc.) was consistently applied. In areas where hybrid assumptions must be made, "engineering judgment" was used to bound expected hybrid potential. For example, a hybrid combustion efficiency of 95% was assumed. Typical state-of-the-art (SOTA) levels are in the range of 87 to 94%. Thus the assumed level is clearly at the upper bounds of expectations, but not beyond the projections anticipated with improved combustion research.

Propellant candidates (derived from industry and PL recommendations) were evaluated on the basis of total loaded impulse. The best propellant combination (PLOX1/BAMO) was carried through to the detailed design and layout analyses. Two cycles, the FIGG and staged combustion gas generator, were considered. The cycles were described in Section 2.2.

The two sets of motors (standard and +15% lengths) for the solid and for the hybrid were "flown" in a series of flight engagement simulations using the OTIS code. The solid systems have the generic boost/sustain thrust profile. The hybrid systems are characterized by two full thrust burns with adjustable dwell times to maximize F-pole range.

After the design effort had been completed, PL asked Chemical Systems Division (CSD) of United Technologies to provide a top-level "sanity check" of the results. CSD indicated that there were no major errors or omissions in the analyses.

The tactical application imposes a much more difficult set of operational and environmental constraints on hardware and consumables (including propellants) than launch vehicle applications. The most notable are wide temperature (typically -65°F to +140°F), low toxicity, and the increasingly stringent thermal and shock limitations (i.e., "insensitive munitions" goals).

The "ideal" hybrid propellant combination would be a suitable solid oxidizer combined with liquid JP fuel (this is known as a reverse hybrid). However, the technology survey was not able to identify any suitable solid oxidizer grains. Thus solid fuels with liquid oxidizers were pursued.

Solid fuels can be grouped into two categories: 1) traditional fuels such as HTPB which cannot sustain combustion without the addition of an oxidizer; 2) gas generator fuels such as glycidl azide polymer (GAP), glycidl azide-A polymer (GAP-A) and BAMO, which all produce fuel-rich gases at relatively low flame temperatures without the aid of added oxidizer. There is an encouraging prospect that the gas generator fuels, which are capable of burn rates an order of magnitude higher than HTPB, will satisfy hazard classification goals (e.g., Class 1.4).

The technology challenge is to identify high-energy, stable, dense liquid oxidizers. Traditional liquids include inhibited red fuming nitric acid (IRFNA), nitrogen tetroxide (NTO), hydrogen peroxide ( $H_2O_2$ ), and nitrous oxide ( $N_2O$ ). These have toxicity, volatility, stability, and performance issues. To meet operational constraints, the IRFNA is gelled, which reduces Isp by a few seconds and could introduce injector clogging concerns for systems that are shut down and restarted.

For volume constrained systems, the most relevant figure-of-merit is the density-specific impulse product (called density impulse). Tables 1 and 2 show a series of propellant combinations that have been optimized for density impulse. In most cases, the density impulse optimum occurs near the Isp optimum. The top three candidates (shown in the table by bold) were further evaluated by performing a preliminary packaging analysis (see Section 4.3 – Design Configurations) to determine the total impulse. The preliminary estimates from Section 4.3 were refined, and a summary of total packaged impulse (given in Table 3) was computed. Note that these values differ slightly from the values in Section 4.3. The refined thrust and Isp calculations were expanded as a function of altitude and used in the engagement analyses discussed in Section 4.4.

**Table 1. Oxidizers and Fuel Densities**

<b>Propellants</b>	<b>Density (g/cc)</b>
<b>Oxidizers</b>	
IRFNA	1.564
$N_2O$	0.510
$NH_4NO_3$	1.725
$N_2O-NH_4NO_3$	0.883
NTO	1.431
HAN (Pure)	1.810
HAN (20% $H_2O$ )	1.560
$H_2O_2$ (Pure)	1.442
$H_2O_2$ (10% $H_2O$ )	1.387
<b>Fuels</b>	
GAP-A	1.240
THF-BAMO (90-10)	0.925
BAMO	1.450
HTPB	0.900

**Table 2. Impulse and Density Impulse for Candidate Tactical Hybrid Systems**

PROPELLANT COMBINATION	MR (O/F)	$\rho_{\text{bulk}}$ (g/cc)	$I_{\text{sp vac}}$ (sec)	$\rho I_{\text{sp vac}}$ (sec*g/cc)
IRFNA/GAP-A	1.250	1.401	288.8	404.7
	1.500	1.416	292.3	413.9
	2.000	1.439	284.6	409.5
N <sub>2</sub> O/BAMO	2.000	0.651	283.8	184.6
	2.500	0.626	288.7	180.7
	3.000	0.609	290.8	177.0
	3.500	0.596	288.5	171.9
NH <sub>4</sub> NO <sub>3</sub> /BAMO	4.000	1.662	251.0	417.2
	5.000	1.672	253.2	423.4
	6.000	1.679	254.5	427.4
	7.000	1.685	248.1	418.1
IRFNA/BAMO	1.500	1.516	290.6	440.6
	1.750	1.521	292.6	444.9
	2.000	1.524	289.6	441.4
NTO/BAMO	1.250	1.439	301.4	433.8
	1.500	1.439	303.8	437.0
	1.750	1.438	300.5	432.1
HAN(PURE)/BAMO	3.000	1.704	276.7	471.6
	3.500	1.715	278.4	477.6
	4.000	1.724	274.1	472.7
HAN (20% H <sub>2</sub> O)/BAMO	3.600	1.535	254.1	390.0
	4.200	1.538	255.7	393.2
	4.800	1.540	251.0	386.5
H <sub>2</sub> O <sub>2</sub> (PURE)/BAMO	2.000	1.445	300.9	434.7
	2.500	1.444	303.5	438.3
	3.000	1.444	296.4	428.0
H <sub>2</sub> O <sub>2</sub> (10% H <sub>2</sub> O)/BAMO	2.200	1.406	290.6	408.6
	2.750	1.403	293.7	412.1
	3.300	1.401	285.9	400.6

( $P_c=1000$  psia,  $P_e=14.7$  psia)

For the purpose of this study, a notional oxidizer, PLOX1, was used with BAMO as the highest performing option, as shown Table 3. This hybrid's total impulse exceeded the solid baselines for both the standard and +15% lengths. The operating points for each propellant combination are given in Table 4. The mixture ratio (MR) was selected at peak density impulse. Chamber pressure and area ratio were based on envelope and structural considerations. The motor designs that were generated (and reported in Section 4.3) were based on these operating points with the best propellant combination, i.e., PLOX1/BAMO. No effort was made to optimize thrust, chamber pressure ( $P_c$ ), MR, and area ratio. It would be expected that some additional performance gains (as measured by mission capability) should be possible.

**Table 3. Summary of Packaged Total Impulse**

Configuration	Propellant	Sea Level Total Impulse (lb-sec)		
		Solid	FIGG Hyb	Stg Comb Hyb
Std Length	PLOX1/BAMO	N/A	27,200	27,900
"	IRFNA/BAMO	N/A	24,400	25,600
"	NTO/BAMO	N/A	24,200	25,500
"	PLOX1/BAMO	N/A	25,400	26,300
"	IRFNA/GAP-A	N/A	21,700	23,200
+15%	PLOX1/BAMO	N/A	33,000	33,700

**Table 4. Candidate Propellant Operating Points**

Configuration	Propellant	PC PSIA	MR O/F	Prop WT LB	Dt IN	De IN	TH VAC Isp sec	TH c* ft/sec	EPS
FIGG/STD LEN	PLOX1/BAMO	1300	3.7	111	1.9	6.0	294	5333	10
FIGG/STD LEN	IRFNA/BAMO	1300	1.750	99	1.9	6.0	293	5306	10
FIGG/STD LEN	NTO/BAMO	1300	1.500	95	1.9	6.0	305	5500	10
FIGG/STD LEN	PLOX1/GAP-A	1300	3.150	103	1.9	6.0	294	5362	10
FIGG/STD LEN	IRFNA/GAP-A	1300	1.500	88	1.9	6.0	293	5343	10
FIGG/+15% LEN	PLOX1/BAMO	1300	3.7	134	1.9	6.0	294	5333	10
STG COMB/STD LEN	PLOX1/BAMO	1300	3.7	113	1.9	6.0	294	5333	10
STG COMB/STD LEN	IRFNA/BAMO	1300	1.750	104	1.9	6.0	293	5306	10
STG COMB/STD LEN	NTO/BAMO	1300	1.500	100	1.9	6.0	305	5500	10
STG COMB/STD LEN	PLOX1/GAP-A	1300	3.150	107	1.9	6.0	294	5362	10
STG COMB/STD LEN	IRFNA/GAP-A	1300	1.500	95	1.9	6.0	293	5343	10
STG COMB/+15% LE	PLOX1/BAMO	1300	3.7	137	1.9	6.0	294	5333	10

Table 3 also shows that there is little difference in packaged impulse (perhaps 2 to 3%) between the classical (actually FIGG, since the BAMO fuel is used) and the staged combustion cycles. That level of discrimination is considered beyond the fidelity of the study.

The advantages of the hybrid concept include the ability to throttle and shut down. However, propellant (burn rate exponent and MR) and cycle selection impacts those abilities. The summaries of shutdown and throttling behavior for the classical, gas generator (staged combustion), and FIGG cycles are given in Figures 8 through 10. In general, the classical is easy to shut down, but suffers from MR excursions as the burn progresses (because of a port area increase) and when throttled (because of a low effective burn rate exponent). On the other hand, the gas generator suffers no MR excursion during burn (assuming constant burn area) and much lower MR excursion during throttling (because of its high burn rate exponent). However, shutdown can be a problem. It is possible to choke across the downstream oxidizer injector, thus preventing sufficient venting to low enough pressures for solid grain extinguishment. The FIGG cycle combines the best of both: it is easy to shut down (like the classical), and has low MR excursion during burn or throttling (like the gas generator).

- Shutdown:
  - Shut Off Oxidizer Flow, Fuel Grain Extinguishes
  - Minimal Cook-off
- MR Shifts
  - MR Increases Even with Constant Burn Surface Area Due to Port Area Changes

$$\frac{MR}{MR_{NOM}} \sim \left( \frac{A_p}{A_{p_{NOM}}} \right)^n$$

$$\text{— Example: } \frac{A_p}{A_{p_{NOM}}} \approx 2 \Rightarrow \frac{MR}{MR_{NOM}} = 1.4$$

- Throttling Results in Decreasing MR

$$\frac{MR}{MR_{NOM}} \sim \left( \frac{P_c}{P_{c_{NOM}}} \right)^n$$

$$\text{— Example: } 9/1 \text{ Throttling} \Rightarrow MR/MR_{NOM} = 0.35$$

**Figure 8**  
**Classical Cycle Shutdown And Throttling**

- Shutdown:
  - Terminating Oxidizer Flow May Not Terminate GG Fuel Grain Combustion
  - $\frac{P_{GG}}{P_{GG_{NOM}}} = \text{Function}(GG \Delta P_{INJ}, n) = \left( \frac{A^*}{A} \right)^{\frac{1}{1-n}}$

$\frac{\Delta P_{INJ}}{P_c}, \%$	$\frac{A^*}{A}$	$\frac{P_{GG}}{P_{GG_{NOM}}}$
5.7	0.485	0.008
10.4	0.621	0.042
* 16.6	0.741	0.135

\* Typical Min  $\Delta P/P_c$  For Tapoff Liquid Pressurization

- MR Shifts
  - None For Constant Thrust Burn With Constant Burn Area
  - Throttling Decreases MR

$$\frac{MR}{MR_{NOM}} \sim \left( \frac{P_c}{P_{c_{NOM}}} \right)^{1-n}$$

$$\text{— Example: } 9/1 \text{ Throttling} \Rightarrow MR/MR_{NOM} = 0.72$$

Relationships in the above figures are for approximation purposes to illuminate critical areas of concern in a system cycle.

**Figure 9**  
**Gas Generator Cycle Shutdown And Throttling**

- Shutdown
  - Shutting Off Oxidizer Reduces GG Pressure
  - Pressure Below Flameout Limits
- MR Shifts
  - Constant Thrust Burn : Like Staged Combustion, i.e. No Shift (Assuming Constant Burn Area)
  - Throttling: Like Staged Combustion, i.e. MR Decreases With Throttling

$$\frac{MR}{MR_{NOM}} \sim \left( \frac{P_c}{P_{cNOM}} \right)^{1-n}$$

— Example Comparison For 9/1 Throttling

<u>SYSTEM</u>	<u>MR/MR<sub>NOM</sub></u>
Classical Cycle	0.35
FIGG Cycle	0.72

Relationships in the above figures are for approximation purposes to illuminate critical areas of concern in a system cycle.

**Figure 10**  
**FIGG Cycle Shutdown And Throttling**

### 4.3 Design Configurations

**4.3.1 Design Considerations.** There are currently two hybrid propulsion cycles that are dominant in the United States at this time: the classical hybrid and the staged combustion hybrid. Each cycle operates on an entirely different approach and has its own unique advantages and disadvantages. Based on propellant availability (Section 4.2 – Tactical Missile Hybrid Technology Study Section), only hybrids using a liquid oxidizer and a solid fuel grain were considered.

The classical hybrid is considered to be the more simple of the two hybrid cycles. It operates by injecting the liquid oxidizer into the cavity of the solid fuel grain. During startup, there is a timed release of a pyrophoric material into the solid fuel cavity followed in a few milliseconds by injection of the liquid oxidizer. When all three come into contact, ignition begins and a process of fuel vaporization sustains combustion within the solid fuel grain cavity. During the combustion process the fuel is continuously vaporized from the grain surface and mixed in a combustion zone above the fuel surface. Within this zone are areas of varying mixture ratio. The complete combustion process takes place along the length of the grain cavity. It is assumed that additional mixing and combustion occurs in the extended nozzle blast tube, which improves combustion efficiency. An important consideration is that the combustion process does not occur in a “constant” environment, i.e., the combustion process occurs in a continuously increasing chamber volume. The classical hybrid can increase thrust by increasing the number of ports available for the liquid oxidizer spray, although this reduces effective mass fraction.

The staged combustion hybrid operates on a different principal. It utilizes a solid fuel gas generator capable of undergoing a controlled and rapid decomposition, thereby providing a ready source of fuel-rich gas. This decomposition process is initiated by a pyrophoric igniter system. Under adequate pressure the solid material sublimates and goes directly into the gaseous state. The gaseous material is relatively hot, approximately 2,000°F or above, and when properly mixed with the liquid oxidizer, final combustion is completed. The combustion of the hot fuel-rich gases and the



oxidizer occurs in a constant volume combustion chamber similar to that of a liquid rocket engine. In the tactical missile design, this process occurs in the blast tube area of the nozzle assembly. The additional length afforded by the blast tube will help to increase the overall combustion efficiency because of the increased residence time of the combustion process. The injector assembly design for the staged combustion hybrid is more complex than the classical hybrid.

The FIGG cycle, a variation of the classical cycle in which the liquid injection configuration of the classical, is combined with a gas-generator-type solid grain. The benefits and characteristics of the FIGG are also described in Section 4.2 (Tactical Missile Hybrid Technology Study System).

The tactical hybrid propulsion systems described in this study utilize a solid fuel and a liquid oxidizing agent. Two solid fuels were considered. One was BAMO, which in the solid form is reported to be a Class 1.4 inert material capable of providing burn rates equivalent to existing solid propellants and an order of magnitude greater than current conventional hybrid fuel materials. The other solid fuel was GAP-A, another reported Class 1.4 inert material under development by both Rocketdyne and Thiokol. This material is reported to have burn rate characteristics similar to BAMO. During the technology survey, the GAP-A burn rate data was presented: 0.50 in/sec at a pressure of 1,000 psia. From discussions with industry and Phillips Laboratory experts, a burn rate exponent value of 0.85 was selected.

Liquid oxidizers were limited to three: IRFNA, nitrogen tetroxide, and PLOX1. Performance screening was based on theoretical Isp calculations.

In volume limited tactical propulsion systems, liquid pressurization packaging becomes of paramount importance. Variable on-demand pressurization systems (needed for throttling and shutdown) impose severe weight and volume penalties. Since it was determined from engagement analysis (see Section 4.4) that two full thrust burns (without throttling) would achieve most of the possible energy management gains, this design effort focused on providing a suitably matched pressurization system. One promising concept was the use of a small solid propellant gas generator for each burn. This concept proved sound. However, packaging became a problem because too much space was required for each gas generator. Problem areas include physical orientation, material thickness required for structural limits, grain surface area requirements, pressure limits, and oxidizer tank plumbing for each line.

In the final concept, the oxidizer tank served as the storage container for the gas generators. The gas generators required to expel the fluid from the tank were integrated into the tank to improve packaging. Gas generator manufacturing companies indicated that this technique was feasible and had been utilized in other systems. To integrate the gas generators into the forward end of the oxidizer dome, a decision was made to take advantage of the relatively large 7-in diameter of the missile and maximize the surface area for each solid gas generator. This would reduce the length of each grain and improve the packaging efficiency. In addition, each gas generator was sealed in a rubber-type insulation material and separated from each grain by approximately 0.0625-in insulation. No ignition source trades were made. Several different approaches could be utilized; one concept was baselined.

Typically, when two pressure vessels are connected, tolerances in one direction (either radial or axial) are relaxed at the connection point. This design with its small diameter made it difficult to meet this condition without adding weight or increasing volume. Therefore, the attachment was constrained to tight tolerances in both radial and axial directions.

Conversations with aerospace tank manufacturers and a review of the Ballistic Missile Defense Organization (BMDO) activities literature indicated two possible methods for positive liquid expulsion: either a positive expulsion bladder or a piston. The amount of volume needed by a piston and its guide arrangement was too great. Industry experience suggests a design with a metal liner bonded to Kevlar™ insulation for structural and thermal integrity. Further discussions indicated a method was necessary to internally bond the bladder to the inside walls of the oxidizer tank, so that when under positive expulsion the bladder would actually peel away from the tank wall. An area of concern was the tear factor attributable to the corners of the bladder near the gas generators. After liquid flow begins, the bladder tear risk diminishes. The best bladder attachment method is to electron beam weld the aft lip of the bladder assembly to the aft boss flange of the oxidizer tank.



Another area of concern is the liquid heating from the gas generator products. Even though there is no direct contact, these thermal considerations need to be addressed. The manufacturers of the gas generators feel they can provide a relatively cool gas, approximately 2,500°F or lower, as a step toward mitigating thermal insulation requirements.

A critical part of the overall design was development of the injector. A design with only o-ring seals and one primary mating attachment was accomplished using the flanges of the oxidizer tank and the solid motor case as the structure. All internal components must be machined with close tolerances for the o-ring mating concept to be effective.

The injector assemblies were designed to integrate as mated flanged assemblies and fluidically isolated by o-ring seals. The injectors provide a very fine spray into the combustion chamber cavity. Each injector had a series of symmetrically oriented hole patterns combined with a mechanical distribution plate located relatively close to the injector inlet, but upstream to uniformly distribute the spray pattern. Each injector was carefully designed to ensure that proper pressure drop was maintained. Each hybrid concept utilized similar gas generators and oxidizer tank expulsion pressures.

Electric Discharge Machining (EDM) produced very sharp edged holes in the injector faceplate of the FIGG hybrid injector and spoke assemblies of the staged combustion wagon wheel injector. Approaches for each injector varied only in associated pressure budgets. The FIGG injector design was relatively straightforward. The staged combustion injector design was more complex, because it must accommodate oxidizer flow, the space claim of feed tube assembly, and the flow of the decomposed gas from the solid gas generator located in the solid motor case.

Many different valving concepts were evaluated to provide a means of controlling liquid flow from storage tank to the combustion chamber for each pulse. Mechanically and pneumatically operated valves were complex and heavy and required too much internal volume. The final selected concept that would enable liquid transfer and provide the required sealing was compact. A pyrotechnically operated set of slider valves, a sort of flat wafer-type assembly, would fit between both storage vessels. Each slider valve would be controlled by individual pyrotechnic squibs located around the periphery of the valve assembly housing.

**4.3.2 FIGG Cycle Designs (Standard Length).** The FIGG hybrid design consists of a liquid oxidizer, a solid fuel grain, and a conventional spray-type injector located at the head end of the solid fuel grain. This rocket motor utilizes the same envelope as the tactical solid. Other sectional properties, such as nozzle configuration, exit and throat areas, blast tube diameter and length, etc. were held as close as practical.

The FIGG hybrid design is the best candidate selected from a series of trade studies (different propellant combinations). Table 5 lists the propellants considered and their performance parameters.

**Table 5. Performance Results for Candidate Hybrid Rocket Propellants**

<u>Candidate propellant</u>	<u>O/F</u>	<u>Total Impulse (lb-sec)</u>	<u>Mass Fraction</u>
PLOX1/BAMO	3.7	29,500	0.69
IFRNA/BAMO	1.750	26,000	0.67
NTO/BAMO	1.500	25,900	0.66
PLOX1/GAP-A	3.150	27,600	0.68
IRFNA/GAP-A	1.500	23,200	0.64
PLOX1/BAMO (+15%)	3.7	35,900	0.71

The baseline FIGG hybrid configuration selected for the detailed layout is the PLOX1 (oxidizer)/BAMO (solid fuel) hybrid combination. This combination exhibited the highest total impulse and propulsion system mass fraction of the combinations analyzed.

**Material Properties.** The materials selected for the hybrid FIGG tactical missile are listed in Table 6. The basic material selected was 4340 chrome moly steel (a high performance steel with wide application in the aerospace industry). Other materials were selected based on their use in current tactical missile designs. Examples include silica phenolic for the nozzle insulation and Kevlar<sup>TM</sup>-filled ethylene-propylene-unconjugated diene terpolymer (EPDM) insulation for the solid propellant tank insulation.

**Table 6. Materials Used in Construction of Hybrid Rocket Motors**

<u>FIGG</u>	
Oxidizer Tank	4340 chrome moly steel
Liner	Aluminum
Insulation	Kevlar <sup>TM</sup>
Oxidizer	PLOX1
Pressurization System	Solid Propellant
Flow control valve	4340 chrome moly steel
Fuel tank	4340 chrome moly steel
Insulation	Kevlar <sup>TM</sup> -filled EPDM
Propellant	BAMO
Injector	4340 chrome moly steel
Nozzle	4340 chrome moly steel
Insulation	silica phenolic

**Physical Properties.** The overall system length was constrained to 75 in, consistent with the baseline tactical solid rocket motor. Approximately 56% of the length of the rocket motor is utilized by the oxidizer tank. Integral with the oxidizer tank is its pressurization system and the positive expulsion system. The nozzle assembly consists of approximately 21% of the motor overall length with the remaining section consisting of the solid motor case, flow control valve, injector assembly, and secondary ignition system. The nozzle exit diameter is such that when the insulation and nozzle material thickness are included, there is a slight overall decrease in outside diameter from the missile outside diameter, thus forming a slight boat tail at the end of the missile. The summary of the dimensions is given in Table 7.

**Mass Properties.** The mass properties associated with the FIGG hybrid rocket motor are also included in Table 7. The total inert weight of the rocket motor is approximately 48.8 lb. The hybrid motor contains 86.9 lb of liquid oxidizer and 23.6 lb of solid propellant fuel. The total loaded weight for the hybrid motor is approximately 159 lb. The mass fraction of the hybrid is 0.69.

**Table 7. Physical Properties of FIGG Hybrid Rocket Motors**

<u>Physical dimensions</u>	<u>FIGG</u>
Overall propulsion system length, in.	75
Outside diameter, in.	7.0
Oxidizer tank length, in.	42.0
Flow control valve length, in.	1.0
Fuel tank length, in.	17.4
Nozzle assembly length, in.	15.6
Nozzle exit diameter, in.	6.0
Nozzle throat diameter, in.	1.9
<u>Mass</u>	
Pressurization system, lbm	2.5
Oxidizer tank, lbm	21.1
Oxidizer outflow valve, lbm	2.4
Injector, lbm	1.0
Injector distribution plate, lbm	0.1
Fuel tank, lbm	10.3
Propellant insulation, lbm	1.6
Nozzle, lbm	7.0
Nozzle insulation, lbm	1.6
Ignition system, lbm	0.4
External insulation, lbm	0.2
Other, lbm	0.6
Total inert weight, lbm	48.8
Oxidizer, lbm	86.9
Fuel, lbm	23.6
Total loaded weight, lbm	159.3
Mass Fraction	0.69

**Performance.** Table 8 lists the performance parameters for the FIGG hybrid rocket motor. The BAMO solid gas generator fuel is a high burn rate propellant. The only trade was varying the O/F ratio to determine the point of highest density impulse. Thrust level was assumed to be the peak level identified for the baseline solid propellant motor. Nozzle expansion ratios were held constant near the nominal solid baseline value. No studies were conducted to determine the impact of alternate MR, thrust, Pc or nozzle expansion ratio.

**Pressurization.** The pressurization system (shown in Fig. 11 and summarized in Table 8) consists of two solid propellant gas generators co-located within the forward end of the oxidizer tank. Each generator is bonded in place with an inert insulating material and are physically separated by 0.0625-in insulation. Each has an inert wire mesh bonded to the front surface which acts as a hot wire grid for ignition. The propellant has a burn rate of 0.16 in/sec and is made of current gas generator materials. The gas generators ignite and burn at a constant rate, thereby maintaining a constant pressure of 2,000 psia. The generators were individually sized to perform for the duty cycle, i.e., gas generator 1 operates for 60% of the overall missile flight time and gas generator 2 for the remaining 40% of the duty cycle. Gas generator 2 can be ignited immediately after the first gas generator has been emptied, or the guidance system can adjust the timeline for the second burn initiation sequence. Each gas generator has been designed to provide gases at a temperature of approximately 2,500°F. This temperature is consistent with materials selected for

the positive expulsion system. It is assumed that there will be no reaction between the gas generator effluent and the oxidizer during the short heat transfer time across the positive expulsion membrane.

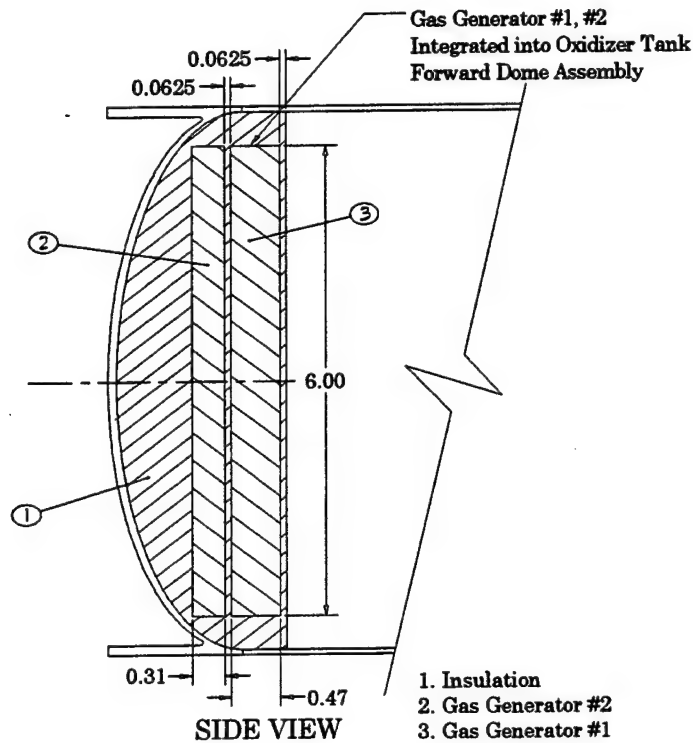


**Figure 11**  
**Standard Length FIGG Hybrid Motor Pressurization System**

**Table 8. FIGG Hybrid Rocket Motor Performance**

<u>Performance Parameter</u>	<u>FIGG</u>
O/F ratio	3.7:1
Chamber pressure, psia	1300
Specific impulse, vac delivered, sec	273
Thrust, vac, lbf	6000
Total impulse, sec	29500
Burn time, sec	4.9
Nozzle expansion ratio	10:1

Pressurization Requirements

<b>Solid Propellant</b>	
Propellant density, lbm/in <sup>3</sup>	0.0635
Combustion temperature, °F	2500
Grain outside diameter, in.	6.0
Grain Surface area, in <sup>2</sup>	28.3
<b>Gas Generator 1</b>	
Burn time, sec	2.9
Required propellant mass, lbm	0.85
Thickness, in.	0.47
Burn rate, in/sec	0.16
<b>Gas Generator 2</b>	
Burn time, sec	2.0
Required propellant mass, lbm	0.56
Thickness, in.	0.31
Burn rate, in/sec	0.16

**Layout.** The layout for the FIGG hybrid motor is shown in Figure 12. Starting from left-to-right, the motor consists of a pressurization system, oxidizer tank, flow control valve and injector assembly, squib ignition system, solid propellant motor and integral nozzle assembly.

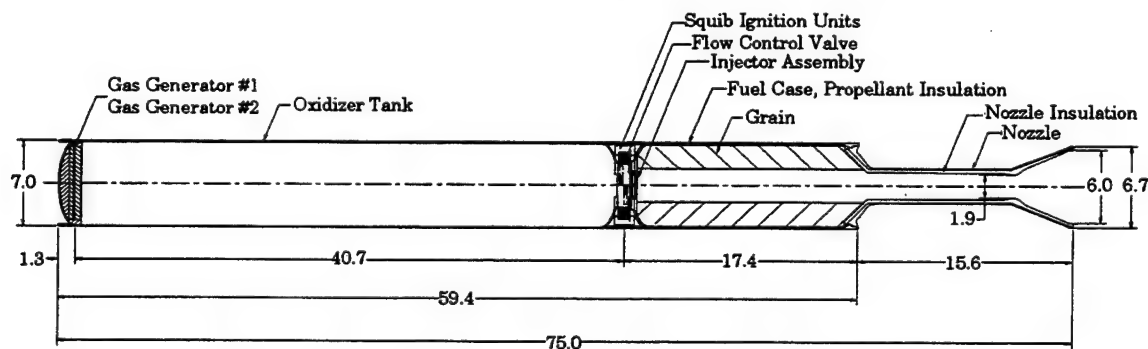


**Figure 12**  
**Standard Length FIGG Hybrid Motor Layout**

**Oxidizer Tank.** The oxidizer tank (shown in Fig. 13 and summarized in Table 9) is designed with 4340 chrome moly steel. It consists of three sections: the forward dome, the cylindrical section, and the aft dome. The overall design of the oxidizer tank utilized a yield safety factor of 1.33 and an ultimate safety factor of 1.65. Both maximum allowables were calculated and the lower value selected for all calculations. The tank was based on ultimate strength. Tank pressure was held at 1,978 psi since the pressure profile for the solid gas generators was constant over the burn time.

The forward dome section was made from a spin formed square root of two ellipsoidal domes with rolled flanges to connect to the forward section of the missile. The cylindrical section consisted of rolled steel welded to the forward dome prior to installing the gas generators. The aft dome was spin formed, with a machined boss at the exit opening and rolled ring flanges to attach it to the aft section of the missile.

The oxidizer system utilized a bonded, metallic rolling bladder design which enabled a propellant utilization of 98%. The bladder consisted of 12- to 20-mil thick aluminum liner with 5 mil of Kevlar™ co-bonded insulation. The bladder assembly was electron-beam (EB) welded to the aft lip of the oxidizer tank.

The tank was constructed such that the forward dome section was welded to the cylindrical section. The gas generator assembly was assembled and machined to fit properly into the forward end of the tank dome, after which it was inserted into the tank and bonded to the forward dome. The cylindrical section was then coated with a very light bonding agent. The bladder (or liner) assembly was EB welded to the aft dome flange lip and inserted deflated on a mandrel into the cylindrical section of the tank. Once in place, the aft dome assembly was welded and the bladder (liner) assembly inflated with gaseous nitrogen to form the bond required for the expulsion system. All electrical connections would be made and all welds X-ray inspected.

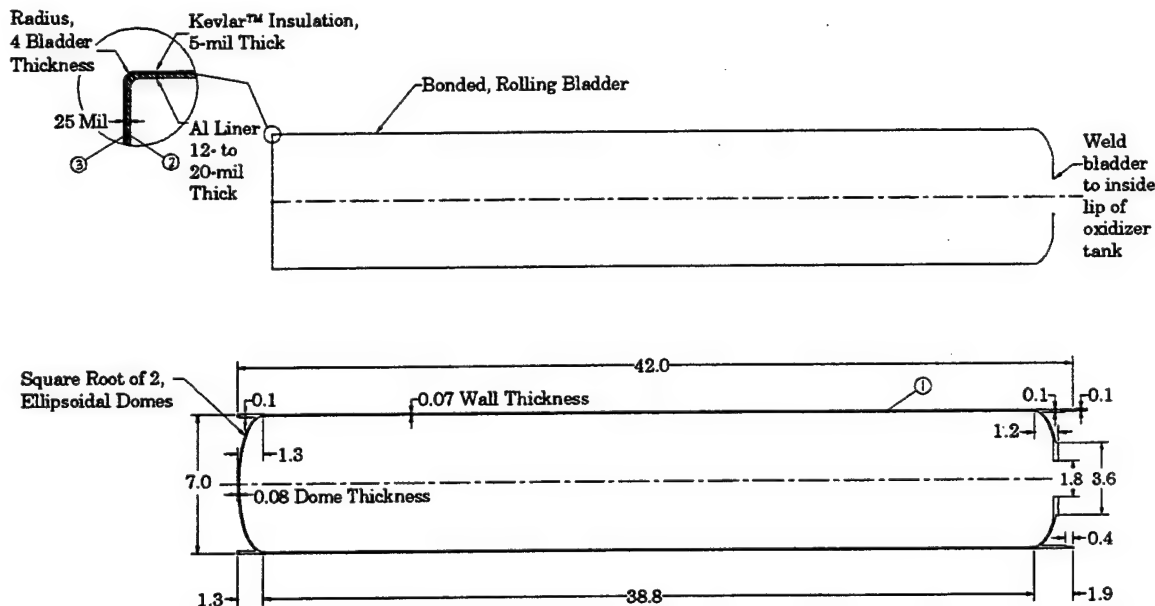


**Figure 13**  
**Standard Length FIGG Hybrid Motor Oxidizer Tank**

**Flow Control Valve.** Since early engagement studies determined that constant thrust for two independent burns delivered good flight performance, a variable delay flow control valve was designed. The flow control valve (shown in Fig. 14 and summarized in Table 9) is a pancake-type device that uses pyrotechnically activated sliding valves to open and close, as required, throughout

the flight profile. Each valve can go from the closed to open position and return to the closed position. The device, machined from 4340 chrome moly steel, is held in place with o-rings forming a seal with the oxidizer tank.

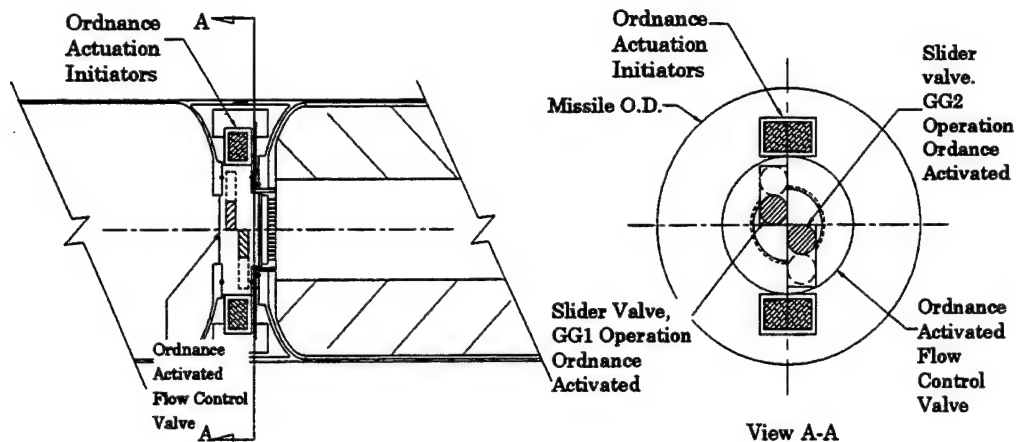


**Figure 14**  
**Standard Length FIGG Hybrid Motor Flow Control Valve**

**Distribution Plate.** The distribution plate (shown in Fig. 15 and summarized in Table 9) creates a pressure drop across the liquid flow from the oxidizer tank. This pressure drop is used to establish a uniform mass flow distribution throughout the injector. The 4340 chrome moly steel distribution plate is sized to withstand a pressure drop of 216.5 psi with a flowrate of 17.3 lbm/sec. A total of 16 equally spaced holes was selected as optimum.

Each hole was assumed to have a discharge coefficient of 0.70, which results in a required diameter of 0.096 in. The distribution plate is inserted into a base flange machined into the injector housing and welded in place.

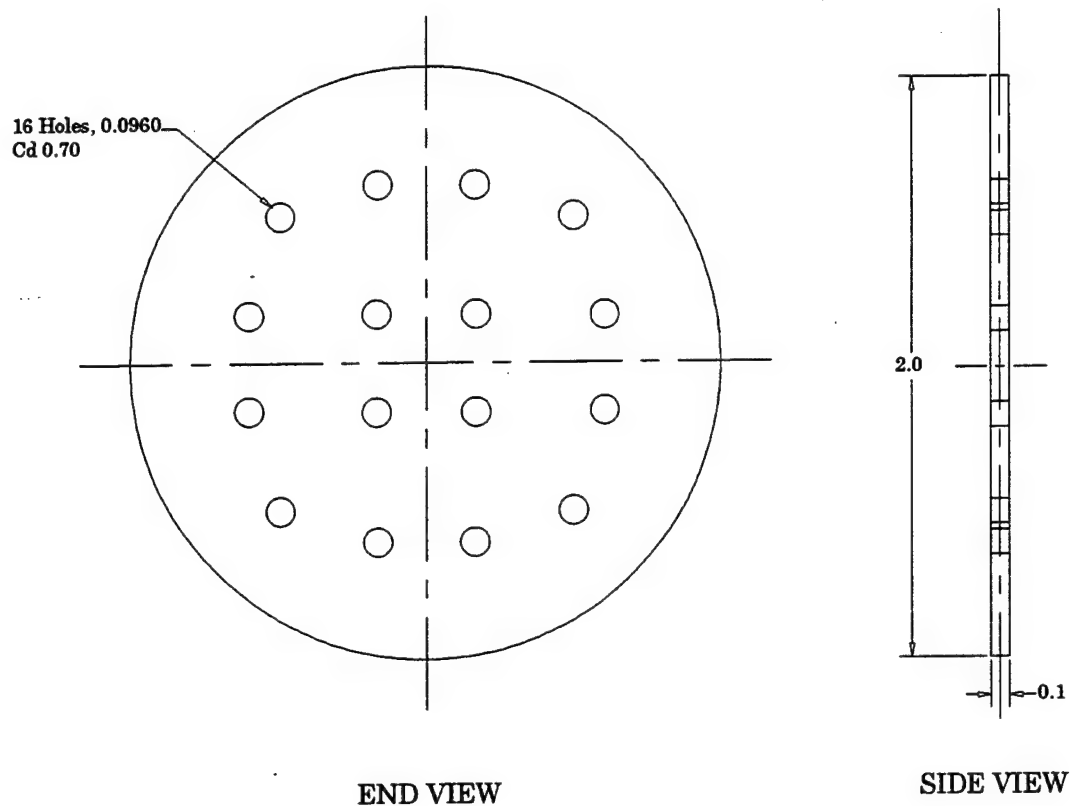


**Figure 15**  
**Standard Length FIGG Hybrid Motor Distribution Plate**

**Injector.** The injector (shown in Fig. 16 and summarized in Table 9) is a one-piece assembly constructed of 4340 chrome moly steel with machined grooves for o-ring fittings which form a positive seal between the flow control valve assembly and the motor case. Machined into opposite ends of the injector are a series of holes that form the flow path for the squib ignition system used during the second ignition.

The injector was sized to handle a pressure drop of 432 psi and a flowrate of 17.3 lbm/sec. The thickness at the injector face is 0.50 in, with an assumed discharge coefficient of 0.90. All 60 holes placed at an angle of  $22.5^\circ$  around the center of the injector face have a 0.037-in diameter. The selected hole pattern was to provide uniform distribution (to maximize combustion efficiency) into the bore of the solid propellant grain. The holes were placed at an angle of  $22.5^\circ$  around the center of the injector face.



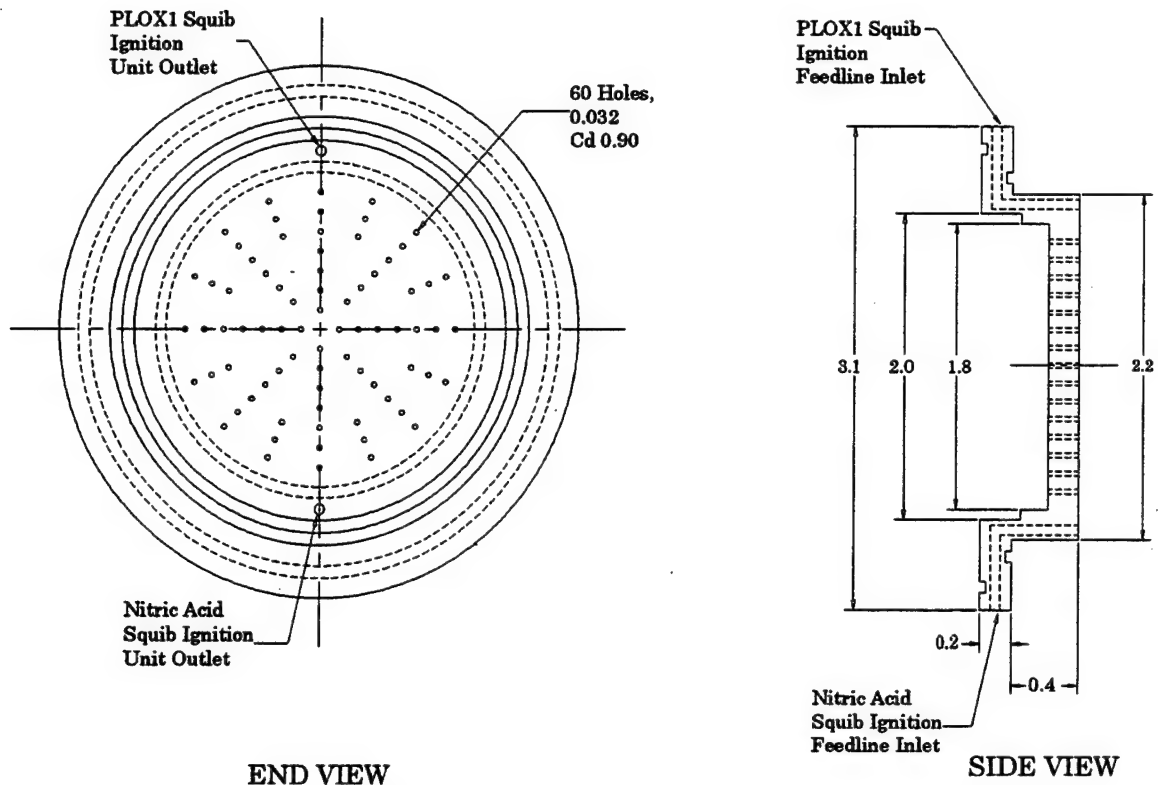


**Figure 16**  
**Standard Length FIGG Hybrid Motor Injector**

**Table 9. Material Properties of Liquid Components of a FIGG HRM**

	<u>FIGG</u>
<u>Oxidizer tank</u> (constructed of chrome moly steel)	
Density, lbm/in <sup>3</sup>	0.285
Yield strength, psi	234000
Safety factor, yield	1.33
Ultimate strength, psi	260000
Safety factor, ultimate	1.65
Weld efficiency, %	100
Tank pressure, psi	1978
Dome type, square root of two, ellipsoidal	
Tank wall thickness, cylindrical section, in.	
Calculated	0.04
Used	0.07
Wall thickness, ellipsoidal dome, in.	
Calculated	0.03
Used	0.08
Expulsion system,	
Type, bonded, metallic rolling bladder	
Efficiency, %	98
Aluminum liner thickness, mils	12 - 20
Kevlar™ insulation thickness, mils	5
<u>Flow control valve</u> , explosive actuation, slider valve)	
Outflow valve	
Diameter, in.	3.5
Thickness, in.	0.9
Mass, lbm	1.8
Ordnance valves	
Volume, in <sup>3</sup>	1.1
Mass, lbm	0.32
Number of Units	2
<u>Distribution plate</u> (constructed of 4340 chrome moly steel)	
Thickness, in.	0.0625
Diameter, in.	2.0
Number of holes	16
Cd, discharge coefficient	0.70
Area per hole, in <sup>2</sup>	0.00727
Diameter per hole, in.	0.0960
Oxidizer	PLOX1
ΔP distribution plate, psi	216
Oxidizer flowrate, lbm/sec	17.3
<u>Injector</u> (constructed of 4340 chrome moly steel)	
Type (Head end conventional spray)	Head end conventional spray
Thickness, in.	0.50
Number of holes	60
Discharge coefficient (Cd)	0.90
Area per hole	0.00107
Diameter per hole, in.	0.0370
Oxidizer type	PLOX1
ΔP, psi	433
Flowrate, lbm/sec	17.3

**Motor Case.** The solid propellant motor case (shown in Fig. 17 and summarized in Table 10) was similar to the oxidizer tank and utilized the same material, 4340 chrome moly steel. The forward dome section is spin formed with rolled ring flanges and contains a machined flange with o-ring grooves for mating with the injector assembly. The forward ring flanges are machined to accept mechanical attachment to the aft ring flange of the oxidizer tank. The proper mating of these two o-ring flange assemblies and the internal mating of the o-ring grooves and o-rings is the most critical part of the fabrication process. The tightest tolerances in the machining process, welding and post machining, will occur here. The forward section is welded to the cylindrical section. The aft dome assembly is then welded to form the complete motor case.

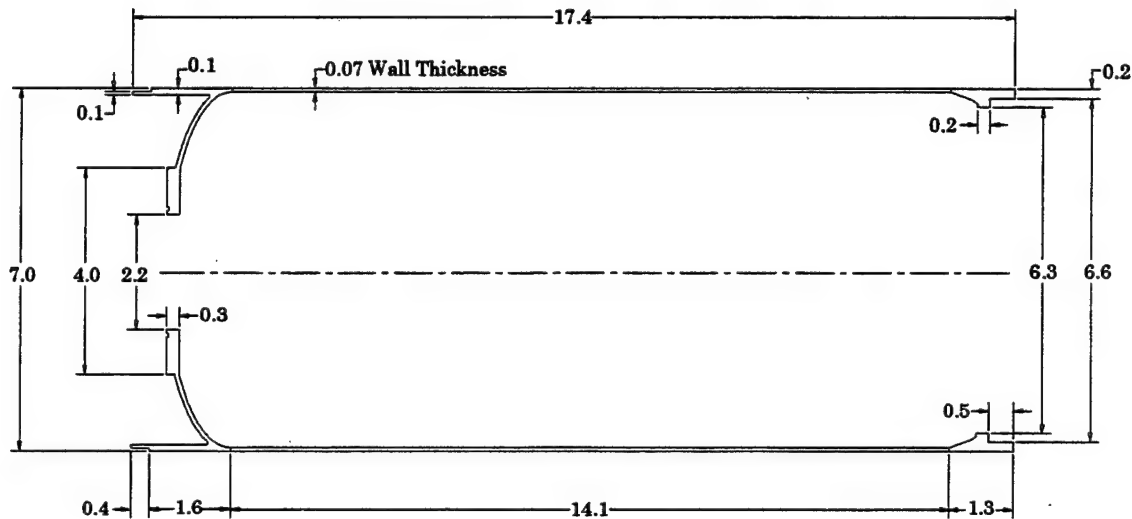


**Figure 17**  
**Standard Length FIGG Hybrid Motor Case**

**Propellant insulation.** The propellant insulation (shown in Fig. 18 and summarized in Table 10) was Kevlar™-filled EPDM. It was bonded into the steel motor case and cured. The insulation thicknesses along the cylindrical and head-end sections of the motor case were sized to be twice that of the solid baseline.

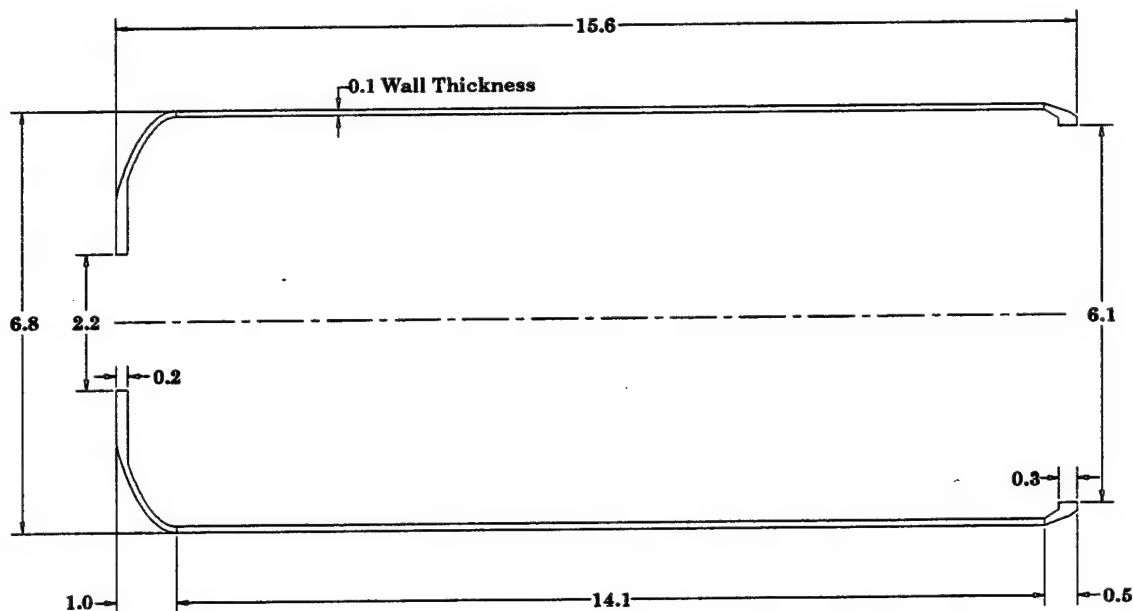


**Figure 18**  
**Standard Length FIGG Hybrid Motor Propellant Insulation**

**Solid Propellant.** The propellant, BAMO, is projected to be a Class 1.4 inert material designed to withstand a controlled gaseous decomposition when ignited at temperatures of 2,000°F and pressures above 150 psi. The propellant has both a high burn rate exponent and a high burn rate. When operated at 1300 psi, its burn rate is estimated to be about 0.62 in/sec. This rate was extrapolated from test data at 1,000 psi.

The propellant (shown in Fig. 19 and summarized in Table 10) is cast into the motor after the propellant insulation is in place. The grain design is a simple cylindrical bore with enough surface area at the BAMO burn rates to produce the desired thrust. No trade studies were conducted to optimize grain design.

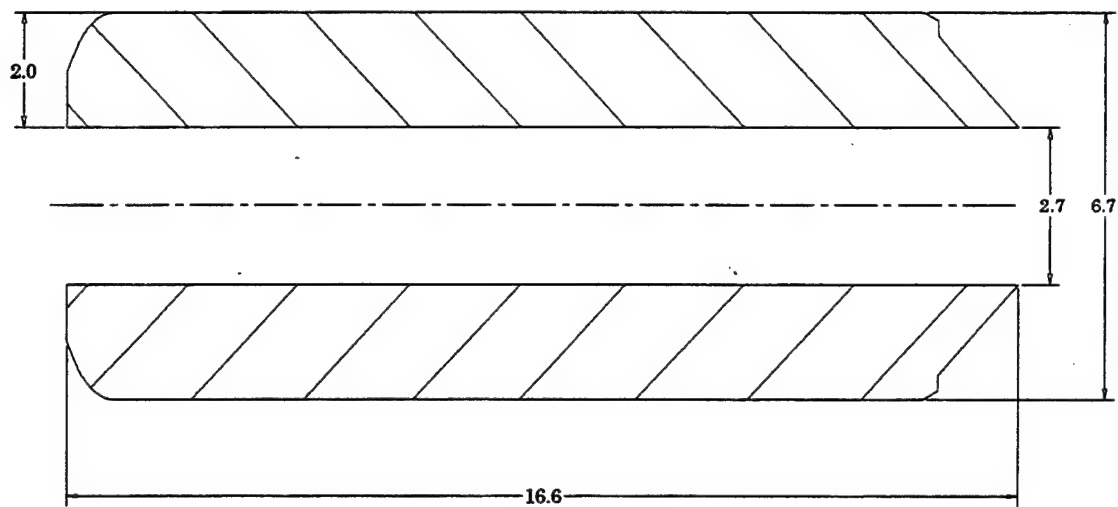


**Figure 19**  
**Standard Length FIGG Hybrid Motor Solid Propellant**

**Nozzle.** The 4340 chrome moly steel nozzle (shown in Fig. 20 and summarized in Table 10) copies the solid baseline nozzle configuration. It is assumed that the nozzle assembly is constructed of three sections: the forward, cylindrical center, and aft. Each section is welded to the next to form the complete nozzle assembly. The nozzle was designed to ensure that the blast tube diameter and overall length corresponded to the solid baseline solid rocket motor (SRM).

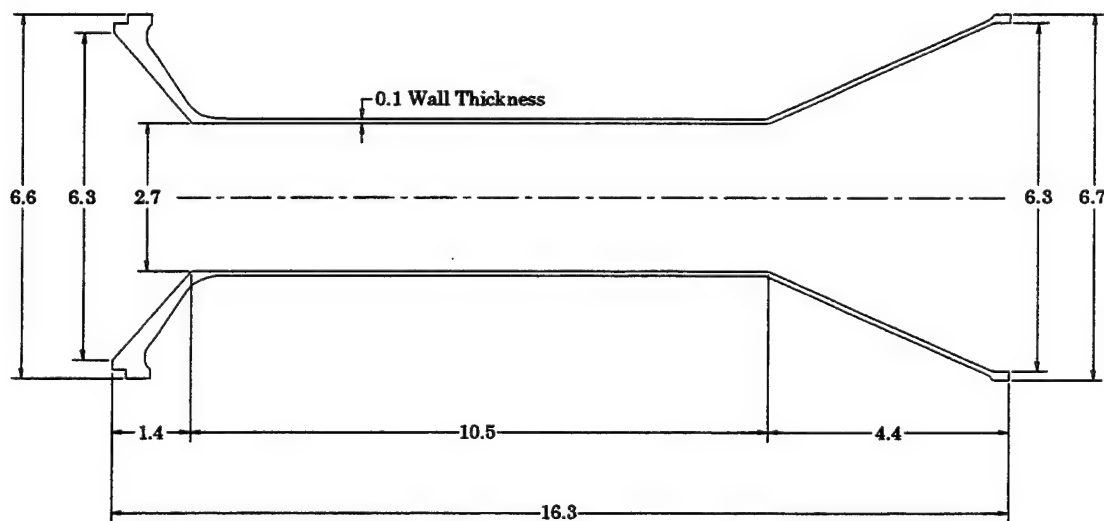


**Figure 20**  
**Standard Length FIGG Hybrid Motor Nozzle**

**Nozzle Insulation.** It is assumed the nozzle insulation (shown in Fig. 21 and summarized in Table 10) is a one-piece casting integral with the steel nozzle housing. Once the insulation material (silica phenolic) is cast, the internal geometry is machined to final dimensions. A wall thickness equivalent to the solid baseline SRM was used. Both nozzle throat and exit areas are established by the propulsion system design.

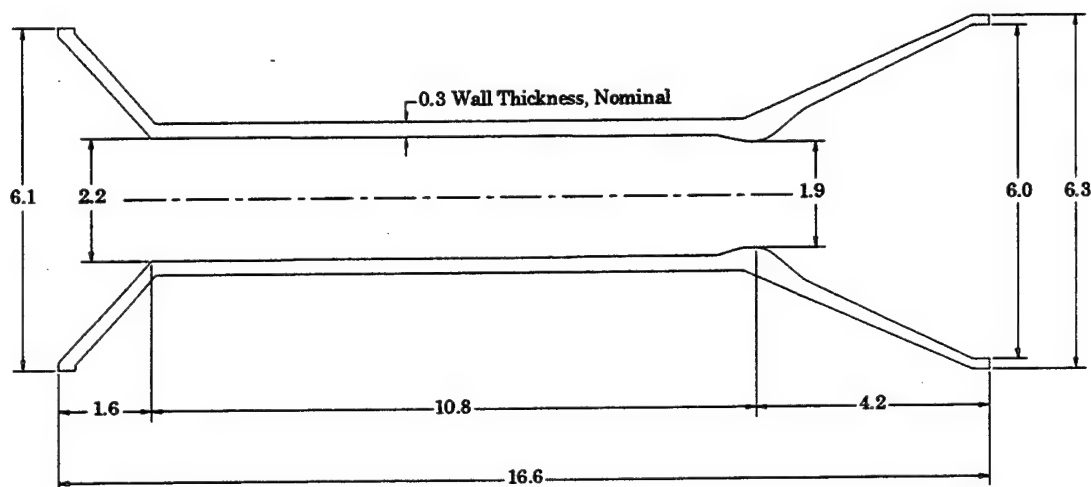


**Figure 21**  
**Standard Length FIGG Hybrid Motor Nozzle Insulation**

**Squib Ignition Unit.** The squib ignition unit (shown in Fig. 22 and summarized in Table 10) is a conceptual design to control ignition at a variable time interval after the termination of the first ignition burn. The concept uses two separate pyrotechnically operated pressure cartridges. When activated, the squib units release 15.0 cc of PLOX1 and nitric acid as a spray into the solid propellant. When mixed, the two liquids would spontaneously ignite. No analysis was conducted to establish threshold limits or liquid quantities required to ensure proper ignition.

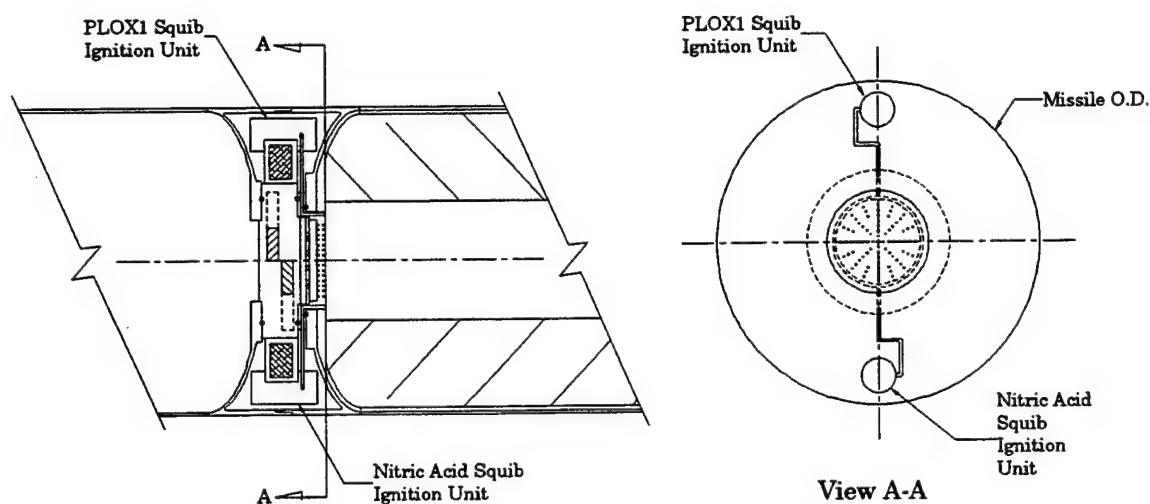


**Figure 22**  
**Standard Length FIGG Hybrid Motor Ignition Unit**

**Table 10. Material Properties of Solid Components of a FIGG HRM**

	<u>FIGG</u>
<u>Solid rocket motor case</u> (constructed of 4340 chrome moly steel)	
Density, lbm/in <sup>3</sup>	0.285
Yield strength, psi	234000
Safety factor, yield	1.33
Ultimate strength, psi	260000
Safety factor, ultimate	1.65
Weld efficiency, %	100
Maximum allowable, yield, psi	175939
Maximum allowable, ultimate, psi	157575
Tank pressure, psi	1300
Dome type, square root of two, ellipsoidal	
Tank wall thickness, cylindrical section, in.	
Calculated	0.03
Used	0.07
Wall thickness, ellipsoidal dome, in.	
Calculated	0.02
Used	0.08
Residual propellant, %	2
<u>Propellant insulation</u> (Kevlar™-filled EPDM)	
Density, lbm/in <sup>3</sup>	0.045
Thickness, cylindrical section, in.	0.1
Thickness, head-end insulation, in.	0.2
Thickness, aft-flap insulation, in.	0.3
<u>Solid Propellant</u> (BAMO)	
Density, lbm/in <sup>3</sup>	0.0524
Burn rate exponent (based on 1000 psi pressure), n	0.85
Burn rate coefficient, (based on 1000 psi pressure), a	0.001409
Pressure, psi	1300
Burn rate, in/sec	0.62
<u>Nozzle</u> (constructed of 4340 chrome moly steel)	
Density, lbm/in <sup>3</sup>	0.285
Wall thickness, nominal, in.	0.08
Maximum diameter, in.	6.7
Maximum length, in.	16.3
<u>Nozzle Insulation</u> (silica phenolic)	
Density, lbm/in <sup>3</sup>	0.0365
Wall thickness, nominal, in.	0.3
Blast tube diameter, inside diameter, in.	2.2
Throat diameter, in.	1.9
Exit diameter, in.	6.0
Combustion gas pressure, psi	1300
Combustion gas temperature, °F	5433
<u>Squib Ignition Unit</u> (second burn ignition system)	
Propellant	PLOX1 and Nitric acid
Ignition source	Hypergolic
Activation	Pyrotechnic
Mass per unit, lbm	0.2

**Missile Configuration.** Figure 23 shows the final integration of the hybrid propulsion system into the missile.

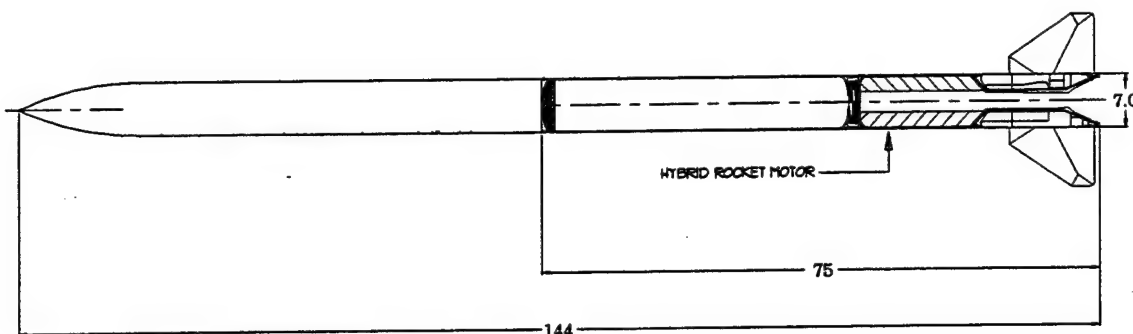


**Figure 23**  
**Standard Length FIGG Hybrid Motor Missile Configuration**

**4.3.3 Staged Combustion Cycle Designs (Standard Length).** The staged combustion hybrid design concept is very similar to the FIGG hybrid design. An effort was made to utilize common methodology. The main difference is in the liquid/solid combustion process. In the FIGG hybrid design the combustion process occurs inside the bore cavity of the solid propellant grain. In the staged combustion cycle, combustion of the liquid occurs in a separate combustion chamber with the gasified fuel-rich products from the gas generator grain. For the staged combustion application, the hot decomposing BAMO gases are directed into the blast tube area of the nozzle assembly. In the process of flowing into the blast tube, the gases pass through a wagon wheel injector where they are mixed with a liquid oxidizer spray. When mixed, the gaseous fuel and the liquid spray undergo spontaneous combustion.

The major benefit of this combustion process is the controlled environment in which the process takes place. In addition, since there is no throttling, mass flowrates are constant. It is assumed that the blast tube is long enough to ensure good combustion.

Those items or effects that are unique to the staged combustion cycle are discussed here. The staged combustion hybrid design evolved from trade studies of several different propellant combinations whose performance is summarized in Table 11. The baseline staged combustion hybrid configuration selected for detailed design is the PLOX1 (oxidizer) and BAMO (solid fuel) hybrid combination because it exhibited the highest total impulse and propulsion mass fraction of the combinations analyzed.

**Table 11. Staged Combustion Hybrid Rocket Performance**

<u>Candidate Propellant</u>	<u>O/F</u>	<u>Total Impulse (lb-sec)</u>	<u>Mass Fraction</u>
PLOX1/BAMO	3.7	30,200	0.69
IFRNA/BAMO	1.750	27,400	0.67
NTO/BAMO	1.500	27,200	0.66
PLOX1/GAP-A	3.150	28,600	0.68
IRFNA/GAP-A	1.500	24,900	0.65
PLOX1/BAMO (+15% Stretch)	3.7	35,500	0.71



**Material Properties.** As shown in Table 12, the staged combustion hybrid oxidizer tank, flow control valve, motor case, and nozzle are constructed of 4340 chrome moly steel. The solid propellant insulation is Kevlar™-filled EPDM, and the nozzle insulation material is silica phenolic.

**Table 12. Materials Used in the Construction of FIGG and SC HRMs**

	<u>FIGG</u>	<u>Staged Combustion HRM</u>
Oxidizer Tank	4340 chrome moly steel	4340 chrome moly steel
Liner	Aluminum	Aluminum
Insulation	Kevlar™	Kevlar™
Oxidizer	PLOX1	PLOX1
Pressurization System	Solid Propellant	Solid Propellant
Flow control valve	4340 chrome moly steel	4340 chrome moly steel
Fuel tank	4340 chrome moly steel	4340 chrome moly steel
Insulation	Kevlar™-filled EPDM	Kevlar™-filled EPDM
Propellant	BAMO	BAMO
Injector	4340 chrome moly steel	4340 chrome moly steel
Nozzle	4340 chrome moly steel	4340 chrome moly steel
Insulation	silica phenolic	silica phenolic

**Physical Properties.** The physical dimensions shown in Table 13 are for the staged combustion baseline configuration. The oxidizer tank utilizes approximately 57% of the total length of the stage combustion hybrid. The nozzle assembly, flow control valve, etc., are representative of the FIGG hybrid design.

**Mass Properties.** Each major section of the staged combustion baseline (summarized in Table 12) is broken down into its elements, and each element has an associated mass property. The total inert weight of the staged combustion hybrid motor is 49.9 lb, approximately 1.0 pound heavier than the FIGG hybrid. The staged combustion hybrid contains 89.0 lb of oxidizer (approximately 2.20 lb more than the FIGG hybrid) and 24.2 lb of solid propellant (approximately 0.6 lb more than the FIGG hybrid). The total loaded weight for the staged combustion hybrid is 163 lb, nearly 4.0 lb heavier than the FIGG hybrid.

The staged combustion hybrid exhibited a slightly higher overall mass fraction than the FIGG hybrid. This was due to the constraint of common combustion pressures and cylindrical bore grain geometry. The FIGG hybrid maintained combustion in the bore of the solid propellant grain, while the staged combustion hybrid would undergo a decomposition in the solid propellant bore at a higher pressure than the FIGG hybrid. The higher pressure would result in a higher decomposition rate, enabling more propellant to be packaged into the motor case of the staged combustion hybrid rocket motor. Final combustion occurs downstream of the wagon wheel injector.

**Table 13. Comparison of Physical Properties of FIGG and SC HRMs**

<u>Physical dimensions</u>	<u>FIGG</u>	<u>Staged Combustion HRM</u>
Overall propulsion system length, in.	75.0	75.0
Outside diameter, in.	7.0	7.0
Oxidizer tank length, in.	42.0	<b>42.9*</b>
Flow control valve length, in.	1.0	1.0
Fuel tank length, in.	17.4	<b>16.5</b>
Nozzle assembly length, in.	15.6	15.6
Nozzle exit diameter, in.	6	6
Nozzle throat diameter, in.	1.9	1.9
<u>Mass</u>		
Pressurization system, lbm	2.5	2.5
Oxidizer tank, lbm	21.1	<b>21.6</b>
Oxidizer outflow valve, lbm	2.4	2.4
Injector, lbm	1.0	<b>1.8</b>
Injector distribution plate, lbm	0.1	0.1
Fuel tank, lbm	10.3	<b>9.9</b>
Propellant insulation, lbm	1.6	<b>1.5</b>
Nozzle, lbm	7.0	<b>7.3</b>
Nozzle insulation, lbm	1.6	1.6
Ignition system, lbm	0.4	0.4
External insulation, lbm	0.2	0.2
Other, lbm	0.6	0.6
Total inert weight, lbm	48.8	<b>49.9</b>
Oxidizer, lbm	86.9	<b>89.0</b>
Fuel, lbm	23.6	<b>24.2</b>
Total loaded weight, lbm	159.3	<b>163.1</b>
Mass Fraction	0.69	0.69

\*Bold print highlights differences

**Performance.** Table 14 enumerates the performance parameters for the staged hybrid rocket motor. Total impulse was higher and the burn time longer than that of the FIGG hybrid. No trades were conducted to determine optimum operating conditions.

**Pressurization.** The pressurization system (shown in Fig. 24 and summarized in Table 14) of the staged combustion hybrid is identical to that of the FIGG hybrid. The staged combustion hybrid's burn times differ slightly.

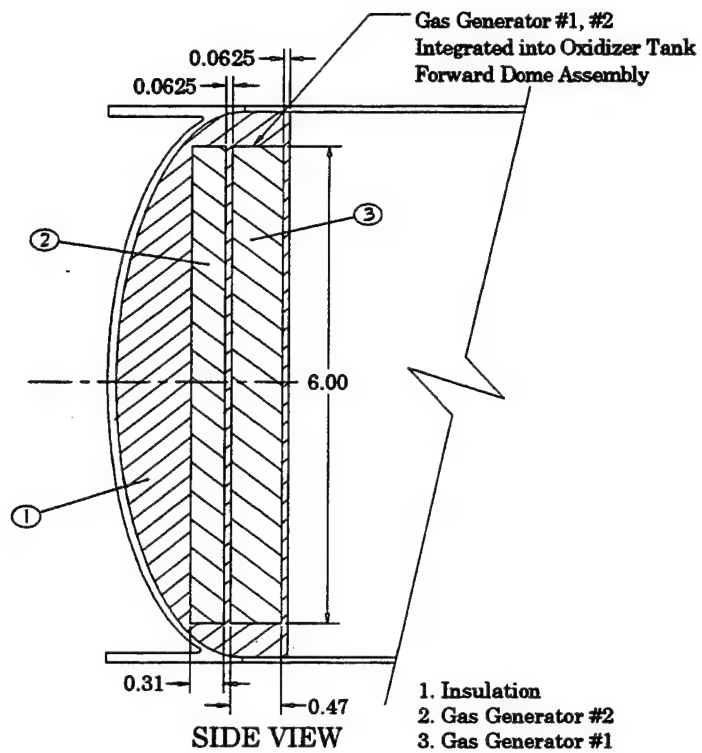


**Figure 24**  
**Standard Length Staged Combustion Hybrid Motor Pressurization System**

**Table 14. Comparison of Hybrid Rocket Motor Performance for FIGG and SC HRMs**

<u>Performance Parameter</u>	<u>FIGG</u>	<u>Staged Combustion HRM</u>
O/F ratio	3.7:1	3.7:1
Chamber pressure, psia	1300	1300
Specific impulse, vac delivered, sec	273	273
Thrust, vac, lbf	6000	6000
Total impulse, sec	29500	<b>30200*</b>
Burn time, sec	4.9	<b>5.0</b>
Nozzle expansion ratio	10:1	10:1

Pressurization Requirements

<b>Solid Propellant</b>		
Propellant density, lbm/in <sup>3</sup>	0.0635	0.0635
Combustion temperature, °F	2500	2500
Grain outside diameter, in.	6.0	6.0
Grain Surface area, in <sup>2</sup>	28.3	28.3
<b>Gas Generator 1</b>		
Burn time, sec	2.9	<b>3.0</b>
Required propellant mass, lbm	0.85	<b>0.87</b>
Thickness, in.	0.47	<b>0.48</b>
Burn rate, in/sec	0.16	0.16
<b>Gas Generator 2</b>		
Burn time, sec	2.0	2.0
Required propellant mass, lbm	0.56	<b>0.58</b>
Thickness, in.	0.31	<b>0.32</b>
Burn rate, in/sec	0.16	0.16

\*Bold print highlights differences

**Layout.** The layout for the staged combustion hybrid is shown in Figure 25. The major difference between the FIGG and staged combustion designs is the injector assembly. The staged combustion injector assembly contains a tube that transfers the oxidizer from the oxidizer tank through the grain cavity to a wagon wheel-type injector.

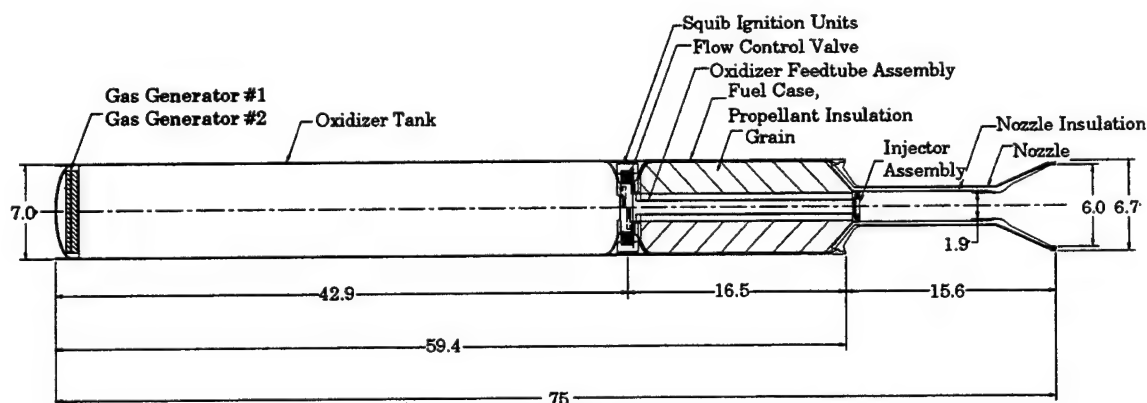


**Figure 25**  
**Standard Length Staged Combustion Hybrid Motor Layout**

**Oxidizer Tank.** The oxidizer tank of the staged combustion hybrid (shown in Fig. 26 and summarized in Table 15) is identical to that of the FIGG hybrid in design and functionality. The cylindrical section of the tank is longer by 1 in. Attachments at both the forward and aft ends are identical and tank construction methodology and techniques are similar. Both a bonded, metallic rolling bladder and attachment of the flow control valve assembly is the same as that of the FIGG.

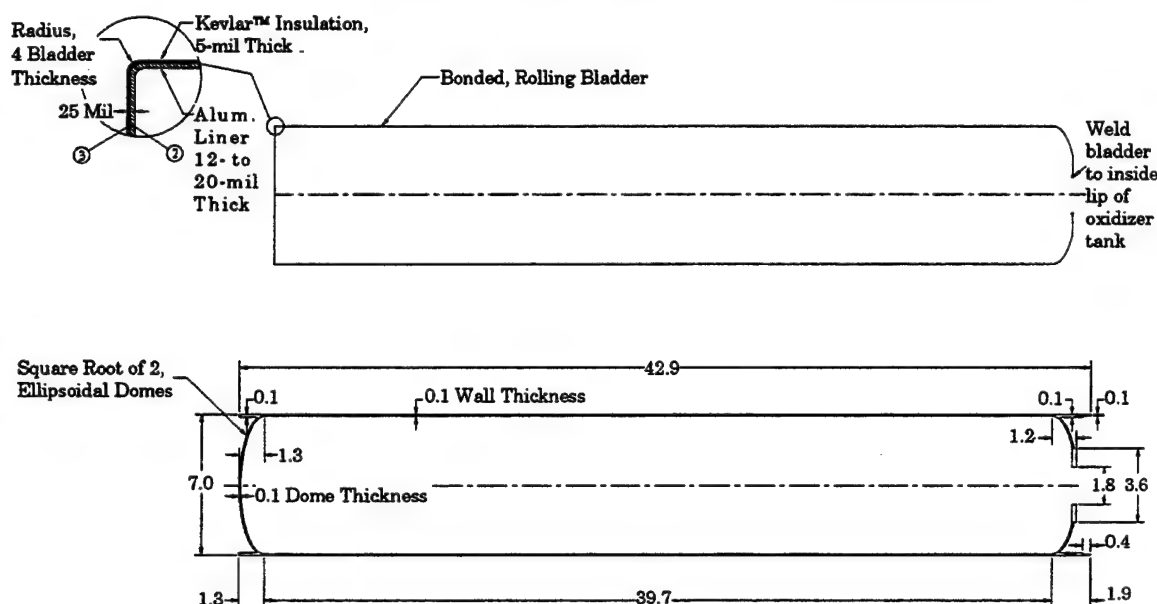


**Figure 26**  
**Standard Length Staged Combustion Hybrid Motor Oxidizer Tank**

**Flow Control Valve.** The flow control valve (shown in Fig. 27 and summarized in Table 15) is identical in both the staged combustion and the FIGG hybrid design concepts.

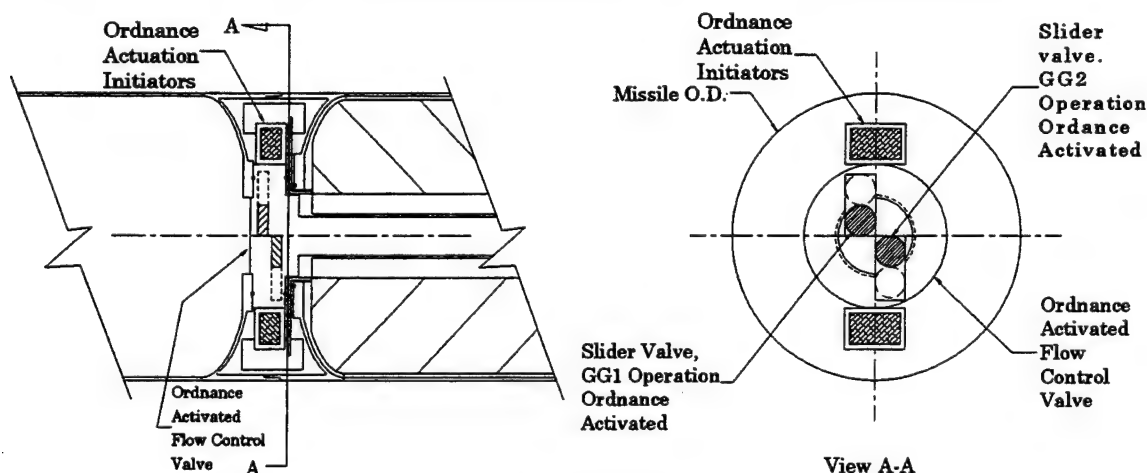


**Figure 27**  
**Standard Length Staged Combustion Hybrid Motor Flow Control Valve**

**Distribution Plate.** The distribution plate for the staged combustion hybrid (shown in Fig. 28 and summarized in Table 15) performs the same function as the FIGG hybrid. The physical location of the device, its diameter, and required pressure drop differ. Both maintain a common operating pressure in the oxidizer tank for each hybrid cycle.

Because the feed tube is located down the center of the solid propellant bore, the distribution plate is located near the outlet of the wagon wheel injector at the aft end of the tube assembly. The 1-in diameter distribution plate has 16 holes 0.117-in diameter symmetrically located on its surface.

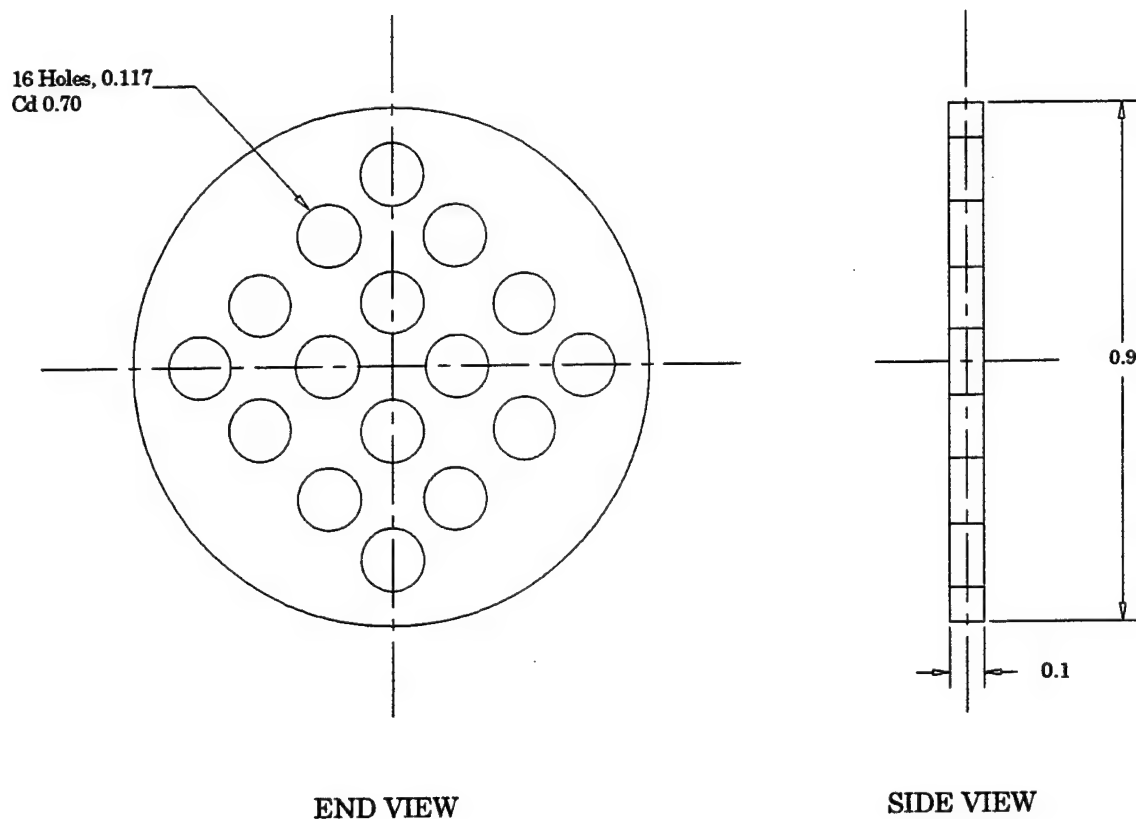


**Figure 28**  
**Standard Length Staged Combustion Hybrid Motor Distribution Plate**

**Injector.** The injector assembly design for the stage combustion hybrid design (shown in Fig. 29 and summarized in Table 15) is considerably different from that of the FIGG hybrid. When solid fuel is ignited, it undergoes a rapid decomposition and provides a relatively hot, high-pressure, fuel-rich gas. When this gas (estimated to be on the order of 2,000°F), mixes with the oxidizer, it spontaneously combusts. The actual combustion process is designed to take place downstream of the aft end of the injector assembly. Added propellant mixing occurs in the blast tube section of the nozzle.

The injector assembly's several sections are welded together to form a monolithic unit. The forward end of the injector assembly is identical to the FIGG hybrid. It utilizes the same boss flanges and o-ring grooves for mating the flow control valve with the solid propellant motor case. A flow tube was created to transfer the fluid from the oxidizer tank to the aft injector. This flow tube is welded to the forward injector flange and integrally mated to the aft injector. The aft injector's distribution plate is designed as a wagon wheel-type spray injector. The spokes of the wagon wheel

act as the flow passage for the oxidizer and have a series of small spray holes on the back side. Each spoke is designed to have hot decomposed gas from the solid propellant gas generator flow past it. When the hot gas flows past the spray holes, the momentum exchange effect helps to further atomize the liquid spray, improving combustion efficiency.

The liquid oxidizer injector was designed for a pressure drop of 195 psi and a liquid oxidizer flowrate of 17.3 lbm/sec. This resulted in spray holes of 0.045 in. in diameter, with five holes located on each of 12 spokes. As part of the liquid injection side there were 12 pie sections made up of the void areas of the wagon wheel. These void areas were used to flow the decomposed gases from the solid propellant gas generator. The gas flow ports (pie sections) were designed to have a pressure drop of 675 psi and flow the decomposed gas at a rate of 4.70 lbm/sec.

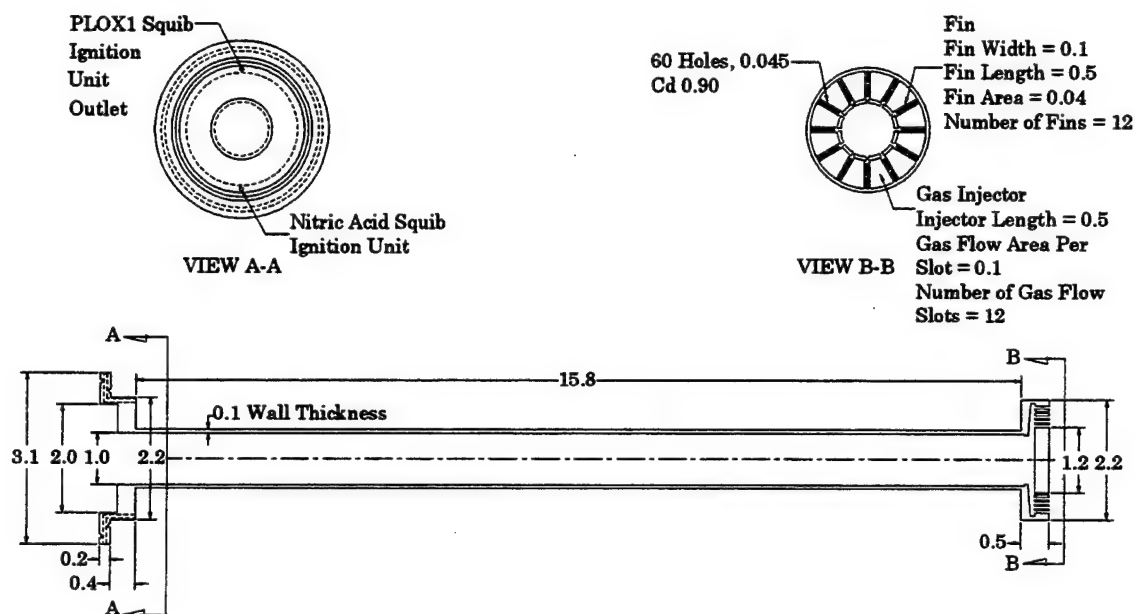


**Figure 29**  
**Standard Length Staged Combustion Hybrid Motor Injector**

**Table 15. Material Properties Comparison of Liquid Components of Two HMRs**

	<u>FIGG</u>	<u>Staged Combustion</u>
<u>Oxidizer Tank</u> (constructed of 4340 chrome moly steel)		
Density, lbm/in <sup>3</sup>	0.285	0.285
Yield strength, psi	234000	234000
Safety factor, yield	1.33	1.33
Ultimate strength, psi	260000	260000
Safety factor, ultimate	1.65	1.65
Weld efficiency, %	100	100
Maximum allowable, yield, psi	175939	175939
Maximum allowable, ultimate, psi	157575	157575
Tank pressure, psi	1978	1975*
Dome type, square root of two, ellipsoidal		
Tank wall thickness, cylindrical section, in.		
Calculated	0.04	0.04
Used	0.07	0.07
Wall thickness, ellipsoidal dome, in.		
Calculated	0.03	0.03
Used	0.08	0.08
Expulsion system,		
Type, bonded, metallic rolling bladder		
Efficiency, %	98	98
Aluminum liner thickness, mils	12 - 20	12 - 20
Kevlar™ insulation thickness, mils	5	5
<u>Flow control valve</u> , (explosive actuation, slider valve)		
Outflow valve		
Diameter, in.	3.5	3.5
Thickness, in.	0.9	1.0
Mass, lbm	1.8	1.8
Ordnance valves		
Volume, in <sup>3</sup>	1.1	1.1
Mass, lbm	0.32	0.32
Number of Units	2	2
<u>Distribution plate</u> (constructed of 4340 chrome moly steel)		
Thickness, in.	0.0625	0.0625
Diameter, in.	2.0	<b>0.9</b>
Number of holes	16	16
Cd, discharge coefficient	0.70	0.70
Area per hole, in <sup>2</sup>	0.00727	<b>0.01084</b>
Diameter per hole, in.	0.0960	<b>0.1170</b>
Oxidizer	PLOX1	PLOX1
ΔP distribution plate, psi	216	<b>98</b>
Oxidizer flowrate, lbm/sec	17.3	17.3
<u>Injector</u> (constructed of 4340 chrome moly steel)		
Type	Head end conventional spray	Aft end radial outflow
Length, in.		15.7897
Thickness, in.	0.50	
Number of holes	60	60
Discharge coefficient (Cd)	0.90	0.90
Area per hole	0.00107	0.00159
Diameter per hole, in.	0.0370	0.0450
Oxidizer type	PLOX1	PLOX1
ΔP, psi	433	195
Flowrate, lbm/sec	17.3	17.3
<u>Gas Injector</u>		
Fuel		BAMO
ΔP, psi		675
Fuel flowrate, lbm/sec		4.7
Flow area, in <sup>2</sup>		1.6
Number of gas ports/fins		12
*Bold print highlights differences		



**Motor Case.** The stage combustion solid propellant motor case (shown in Fig. 30 and summarized in Table 16) construction is identical to that of the FIGG hybrid. The staged combustion cylindrical section is approximately 1 in shorter than that of the FIGG hybrid design.

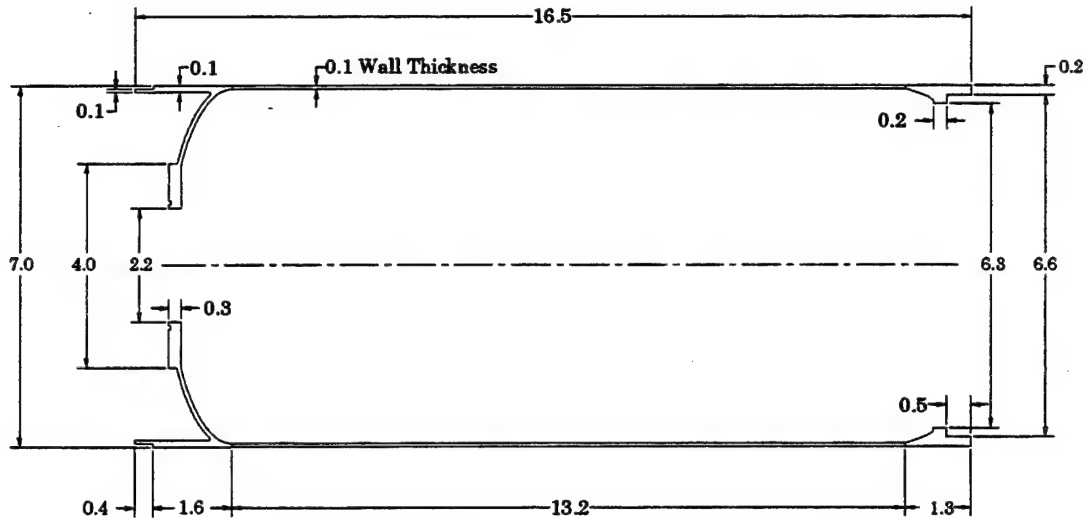


**Figure 30**  
**Standard Length Staged Combustion Hybrid Motor Case**

**Propellant Insulation.** The propellant insulation (shown in Fig. 31 and summarized in Table 16) for the staged combustion hybrid is identical to that of the FIGG hybrid. Both hybrid cycles use the same material, Kevlar<sup>TM</sup>-filled EPDM insulation, but the staged combustion hybrid uses less.

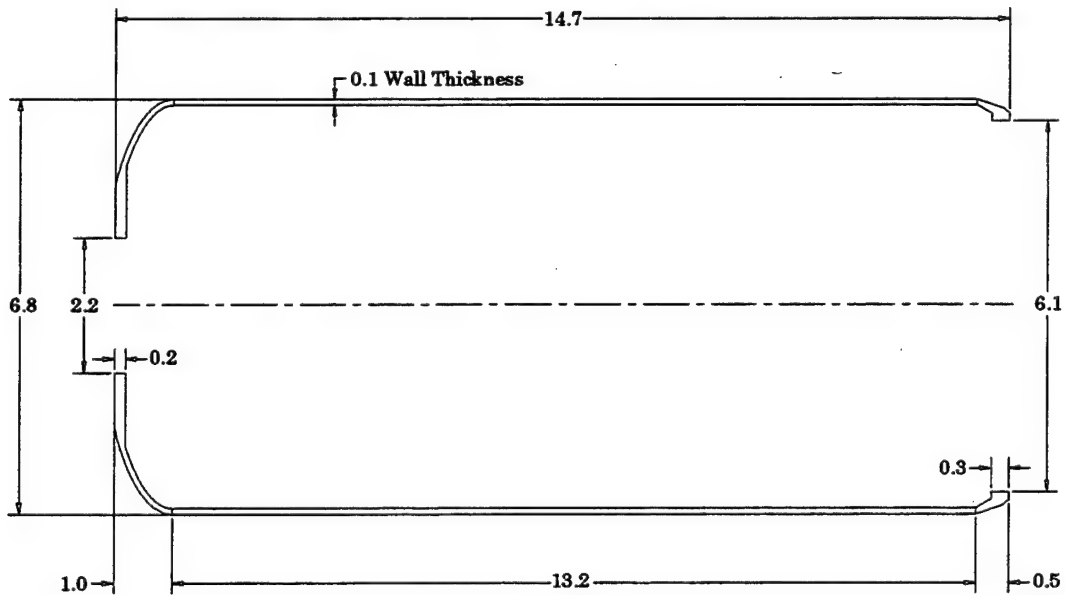


**Figure 31**  
**Standard Length Staged Combustion Hybrid Motor Propellant Insulation**

**Solid Propellant.** The staged combustion hybrid utilizes the same solid propellant as the FIGG hybrid, i.e., BAMO. The FIGG hybrid has a propellant burn rate of 0.62 in/sec based on a chamber pressure of 1,300 psi. In the staged combustion design (shown in Fig. 32 and summarized in Table 16), the operation of the solid gas generator is at a higher pressure. The decomposition rate of the gas generator is 0.9 in/sec, based on a pressure of almost 2,000 psi.

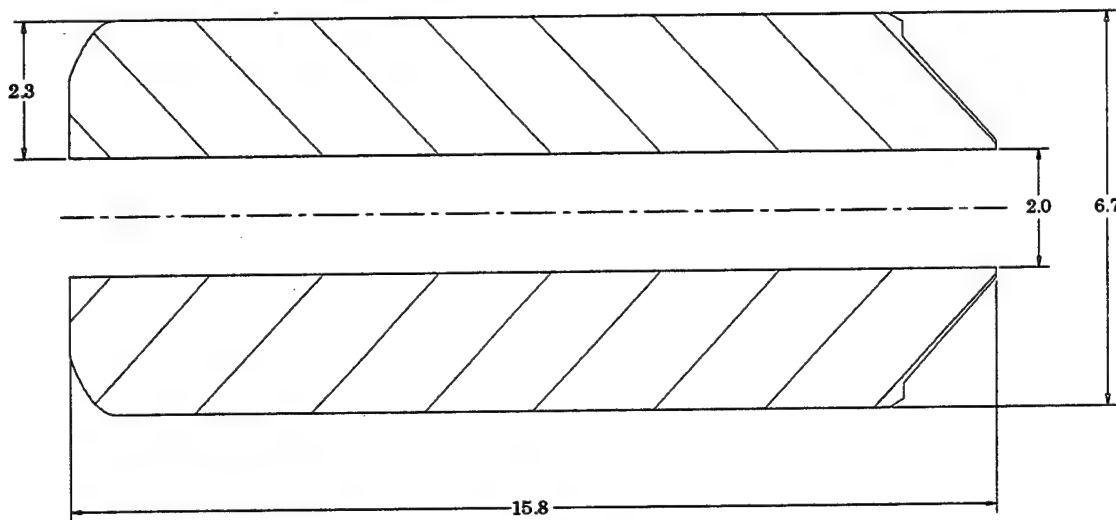


**Figure 32**  
**Standard Length Staged Combustion Hybrid Motor Propellant**

**Nozzle.** The nozzle assembly for the staged combustion hybrid is identical to that of the FIGG hybrid. Material properties, physical dimensions, and assembly techniques are shown in Figure 33 and summarized in Table 16.

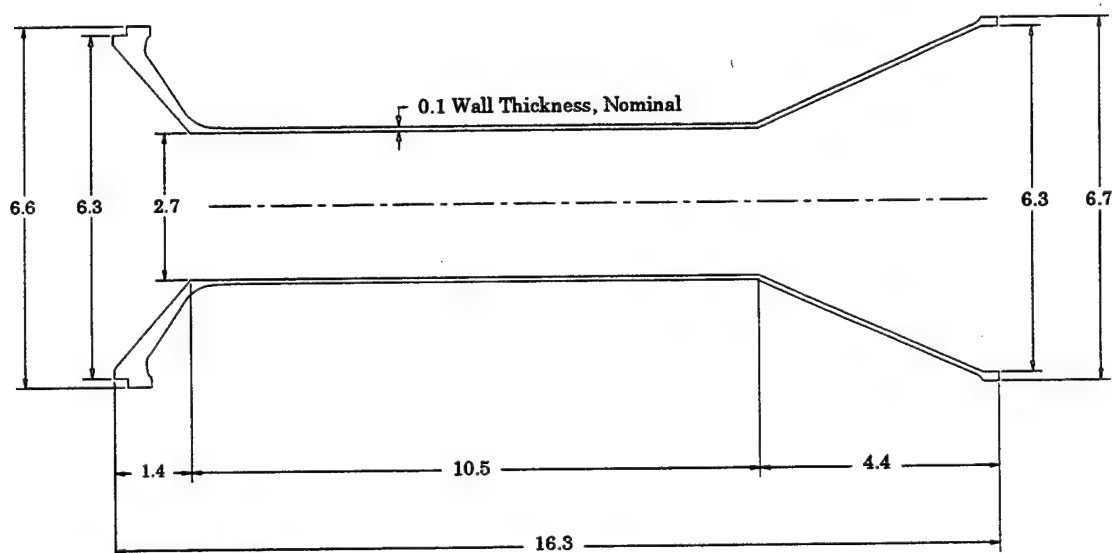


**Figure 33**  
**Standard Length Staged Combustion Hybrid Motor Nozzle**

**Nozzle Insulation.** The design of the nozzle insulation (shown in Fig. 34 and summarized in Table 16) for the staged combustion hybrid is very similar to that of the FIGG hybrid with few exceptions. The forward end of the nozzle insulation forms the interface for the aft end of the injector assembly. The aft end of the injector assembly is free to float in a machined section of the nozzle insulation. The nozzle was designed to provide a free floating area to support the aft injector assembly prior to ignition and then act as a secure physical attachment for the injector when under pressure and high temperature. It was assumed that the injector assembly would have a slight growth when under pressure and high temperature. The machined forward section of the nozzle insulation would be properly designed to control any conditions associated with this phenomenon.

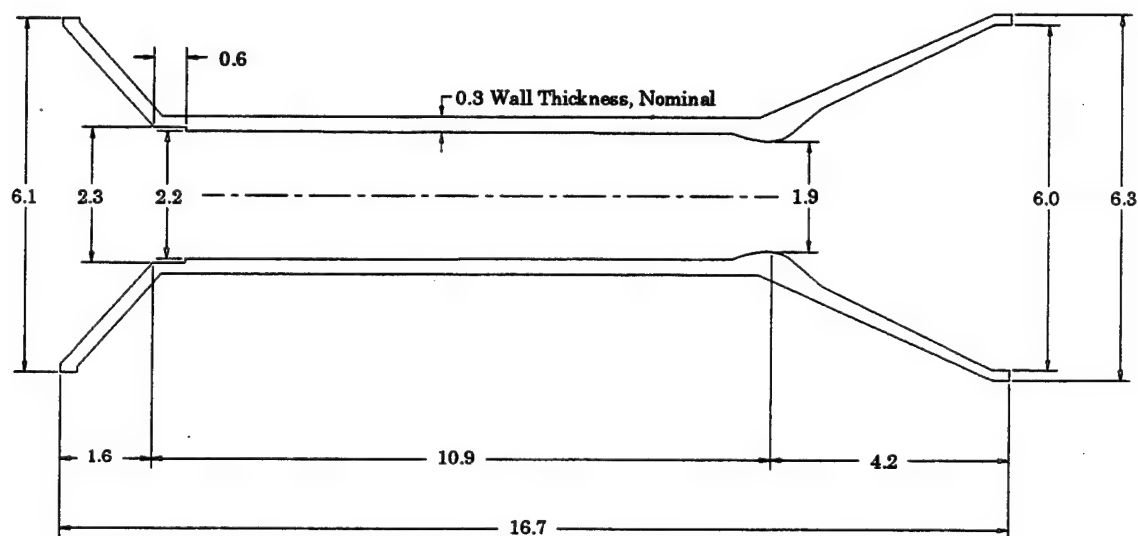


**Figure 34**  
**Standard Length Staged Combustion Hybrid Motor Nozzle Insulation**

**Squib Ignition Unit.** The squib ignition unit (shown in Fig. 35 and summarized in Table 16) is identical in operation to that of the FIGG hybrid.

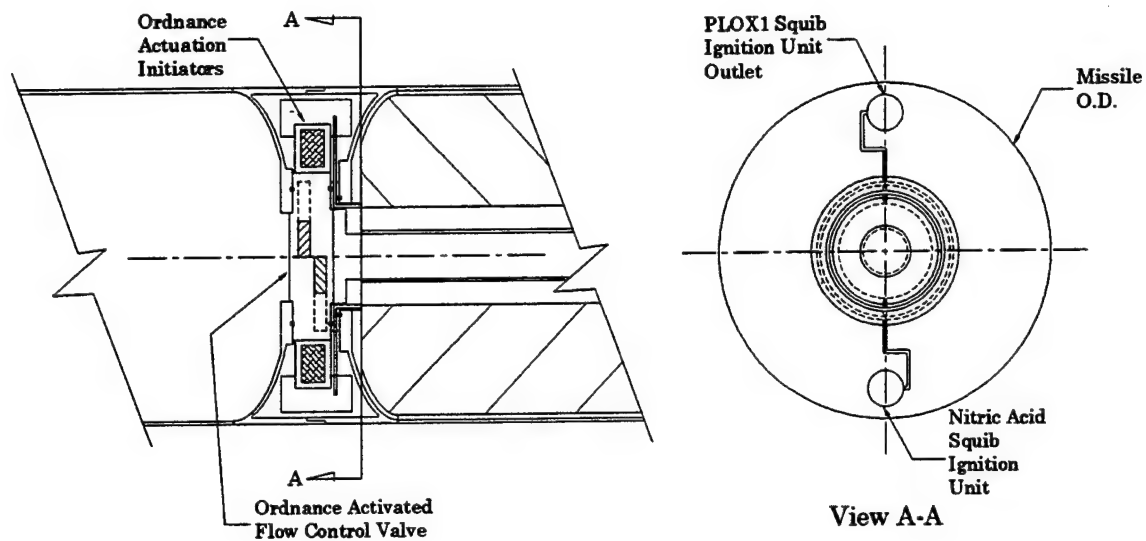


**Figure 35**  
**Standard Length Staged Combustion Hybrid Motor Ignition Unit**

**Table 16. Material Properties of Solid Components of two HRMs**

	<u>FIGG</u>	<u>Staged Combustion</u>
<u>Solid rocket motor case</u> (constructed of 4340 chrome moly steel)		
Density, lbm/in <sup>3</sup>	0.285	0.285
Yield strength, psi	234000	234000
Safety factor, yield	1.33	1.33
Ultimate strength, psi	260000	260000
Safety factor, ultimate	1.65	1.65
Weld efficiency, %	100	100
Maximum allowable, yield, psi	175939	175939
Maximum allowable, ultimate, psi	157575	157575
Tank pressure, psi	1300	1975*
Dome type, square root of two, ellipsoidal		
Tank wall thickness, cylindrical section, in.		
Calculated	0.03	<b>0.04</b>
Used	0.07	0.07
Wall thickness, ellipsoidal dome, in.		
Calculated	0.02	<b>0.03</b>
Used	0.08	0.08
Residual propellant, %	2	2
<u>Propellant insulation</u> (Kevlar™ filled EPDM)		
Density, lbm/in <sup>3</sup>	0.045	0.045
Thickness, cylindrical section, in.	0.1	0.1
Thickness, head-end insulation, in.	0.2	0.2
Thickness, aft-flap insulation, in.	0.3	0.3
<u>Solid Propellant</u> (BAMO)		
Density, lbm/in <sup>3</sup>	0.0524	0.0524
Decomposition gas density, lbm/in <sup>3</sup>		0.000637
Burn rate exponent (based on 1000 psi pressure), n	0.85	0.85
Burn rate coefficient, (based on 1000 psi pressure), a	0.001409	0.001409
Pressure, psi	1300	1975
Burn rate, in/sec	0.62	
Decomposition rate, in/sec		<b>0.9</b>
<u>Nozzle</u> (constructed of 4340 chrome moly steel)		
Density, lbm/in <sup>3</sup>	0.285	0.285
Wall thickness, nominal, in.	0.08	0.8
Maximum diameter, in.	6.7	6.7
Maximum length, in.	16.4	16.4
<u>Nozzle Insulation</u> (silica phenolic)		
Density, lbm/in <sup>3</sup>	0.0365	0.0365
Wall thickness, nominal, in.	0.3	0.3
Blast tube diameter, inside diameter, in.	2.2	2.2
Throat diameter, in.	1.9	1.9
Exit diameter, in.	6.0	6.0
Combustion gas pressure, psi	1300	1300
Combustion gas temperature, °F	5433	5433
<u>Squib Ignition Unit</u> (Second burn ignition system)		
Propellant	PLOX1 and nitric acid	PLOX1 and nitric acid
Ignition source	Hypergolic	Hypergolic
Activation	Pyrotechnic	Pyrotechnic
Mass per unit, lbm	0.2	0.2

\*Bold print highlights differences

**Missile Configuration.** Figure 36 shows the final integration of the staged combustion hybrid rocket motor into the missile. The front ends (guidance, electronics, warhead, etc.) for the staged combustion and FIGG hybrid rocket motors were identical.

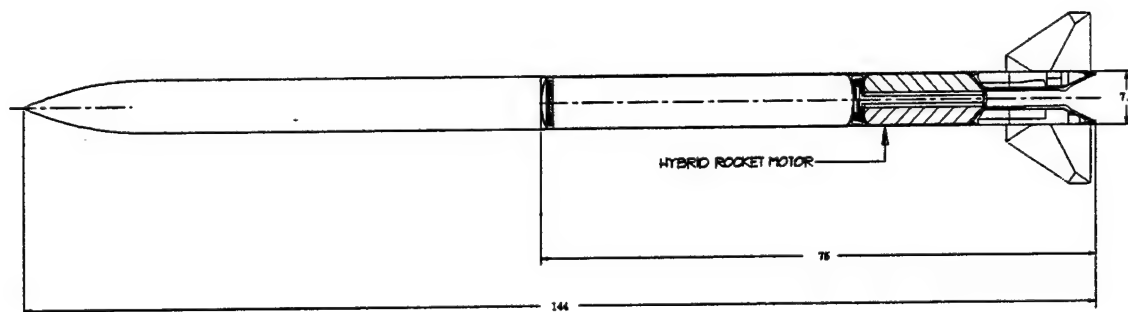


**Figure 36**  
**Standard Length Staged Combustion Hybrid Motor Missile Configuration**

**4.3.4 FIGG Cycle Designs (+15% Length).** The baseline FIGG cycle hybrid rocket motor was stretched +15% and new mass properties and performance numbers were generated. It was assumed that only burn time and propellant load would change, that motor thrust and specific impulse would remain unchanged, and that motor total impulse would increase because of the increased motor burn time and increased propellant load.

**Material Properties.** As shown in Table 17, material properties were identical with those of the baseline FIGG hybrid rocket motor.

**Table 17. Materials Used in the Construction of FIGG and +15% HRMs**

	<u>FIGG</u>	<u>+15% FIGG HRM</u>
Oxidizer Tank	4340 chrome moly steel	4340 chrome moly steel
Liner	Aluminum	Aluminum
Insulation	Kevlar™	Kevlar™
Oxidizer	PLOX1	PLOX1
Pressurization System	Solid Propellant	Solid Propellant
Flow control valve	4340 chrome moly steel	4340 chrome moly steel
Fuel tank	4340 chrome moly steel	4340 chrome moly steel
Insulation	Kevlar™ filled EPDM	Kevlar™ filled EPDM
Propellant	BAMO	BAMO
Injector	4340 chrome moly steel	4340 chrome moly steel
Nozzle	4340 chrome moly steel	4340 chrome moly steel
Insulation	silica phenolic	silica phenolic

**Physical Properties.** The motor propulsion system's overall was increased by +15% (Table 18). This stretch resulted in an 8.6-in oxidizer tank increase and a 2.5-in fuel tank increase. Other physical dimensions for the motor assembly remained unchanged.

**Mass Properties.** Motor mass increased because of the +15% stretch, as shown in Table 18.

**Table 18. Comparison of Physical Properties of FIGG and +15% HRMs**

<u>Physical dimensions</u>	<u>FIGG</u>	<u>+15% HRM</u>
Overall propulsion system length, in.	75.0	<b>86.0*</b>
Outside diameter, in.	7.0	7.0
Oxidizer tank length, in.	42.0	<b>49.5</b>
Flow control valve length, in.	1.0	1.0
Fuel tank length, in.	17.4	<b>19.6</b>
Nozzle assembly length, in.	15.6	15.6
Nozzle exit diameter, in.	6.0	6.0
Nozzle throat diameter, in.	1.9	1.9
<u>Mass</u>		
Pressurization system, lbm	2.5	<b>2.8</b>
Oxidizer tank, lbm	21.1	<b>24.8</b>
Oxidizer outflow valve, lbm	2.4	2.4
Injector, lbm	1.0	1.0
Injector distribution plate, lbm	0.1	0.1
Fuel tank, lbm	10.3	<b>11.4</b>
Propellant insulation, lbm	1.6	<b>1.8</b>
Nozzle, lbm	7.0	7.0
Nozzle insulation, lbm	1.6	1.6
Ignition system, lbm	0.4	0.4
External insulation, lbm	0.2	0.2
Other, lbm	0.6	0.6
Total inert weight, lbm	48.8	<b>54.1</b>
Oxidizer, lbm	86.9	<b>105.6</b>
Fuel, lbm	23.6	<b>28.7</b>
Total loaded weight, lbm	159.3	<b>188.4</b>
Mass Fraction	0.65	<b>0.71</b>

\*Bold print highlights differences

**Performance.** Increasing the motor length +15% increased motor total impulse and burn time, as shown in Table 19.

**Table 19. Comparison of Performance for FIGG and +15% FIGG HRMs**

<u>Performance Parameter</u>	<u>FIGG</u>	<u>+15% FIGG</u>
O/F ratio	3.7:1	3.7:1
Chamber pressure, psia	1300	1300
Specific impulse, vac delivered, sec	273	273
Thrust, vac, lbf	6000	6000
Total impulse, sec	29500	<b>35900*</b>
Burn time, sec	4.9	<b>6.0</b>
Nozzle expansion ratio	10:1	10:1

**Pressurization Requirements**

<b>Solid Propellant</b>		
Propellant density, lbm/in <sup>3</sup>	0.0635	0.0635
Combustion temperature, °F	2500	2500
Grain outside diameter, in.	6.0	6.0
Grain Surface area, in <sup>2</sup>	28.3	28.3
<b>Gas Generator 1</b>		
Burn time, sec	2.9	<b>3.6</b>
Required propellant mass, lbm	0.85	<b>1.03</b>
Thickness, in.	0.47	<b>0.57</b>
Burn rate, in/sec	0.16	0.16
<b>Gas Generator 2</b>		
Burn time, sec	2.0	<b>2.4</b>
Required propellant mass, lbm	0.56	<b>0.68</b>
Thickness, in.	0.31	<b>0.38</b>
Burn rate, in/sec	0.16	0.16

\*Bold print highlights differences

**Layout.** The layout for the +15% stretch FIGG hybrid is shown in Figure 37. The motor assembly is exactly the same as the FIGG hybrid baseline configuration except for the increased length of selected components.

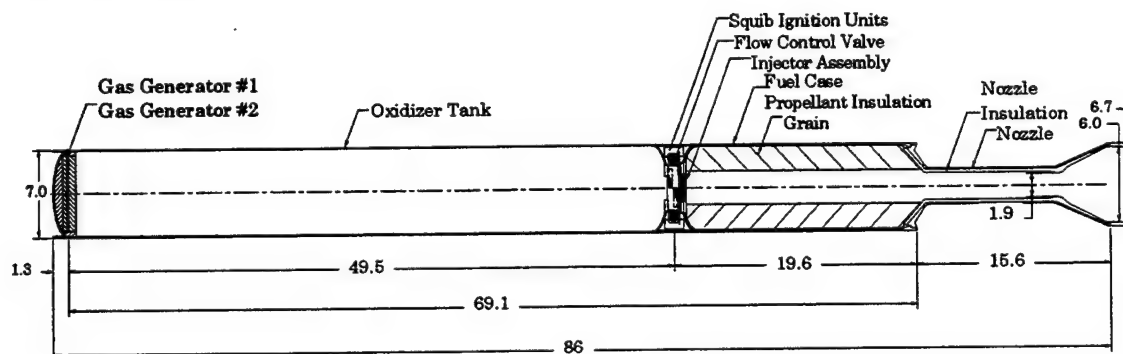


**Figure 37**  
**+15% Length FIGG Hybrid Motor Layout**

**Missile Configuration.** Figure 38 shows all components of the +15% stretch FIGG hybrid rocket motor integrated into the total missile.



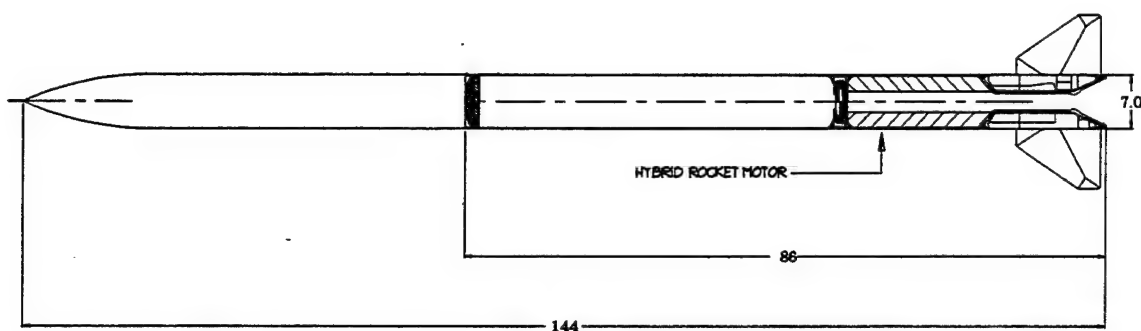


**Figure 38**  
**+15% Length FIGG Hybrid Motor Missile Layout**

**4.3.5 Staged Combustion Cycle Designs (+15% Length).** The baseline staged combustion cycle hybrid rocket motor was stretched +15% and new mass properties and performance numbers were generated. It was assumed that only burn time and propellant load would change and that motor thrust and specific impulse would remain unchanged. Motor total impulse would increase due to the increased motor burn time and increased propellant load.

**Material Properties.** Material properties, as shown in Table 20, remained identical to those of the baseline staged combustion cycle hybrid rocket motor.

**Table 20. Materials Used in Construction of FIGG, +15% FIGG, SC and +15% SC HRMs**

	<u>FIGG or FIGG +15%</u>	<u>Staged Combustion or +15% SC</u>
Oxidizer Tank	4340 chrome moly steel	4340 chrome moly steel
Liner	Aluminum	Aluminum
Insulation	Kevlar™	Kevlar™
Oxidizer	PLOX1	PLOX1
Pressurization System	Solid Propellant	Solid Propellant
Flow control valve	4340 chrome moly steel	4340 chrome moly steel
Fuel tank	4340 chrome moly steel	4340 chrome moly steel
Insulation	Kevlar™ filled EPDM	Kevlar™ filled EPDM
Propellant	BAMO	BAMO
Injector	4340 chrome moly steel	4340 chrome moly steel
Nozzle	4340 chrome moly steel	4340 chrome moly steel
Insulation	silica phenolic	silica phenolic

**Physical Properties.** The motor propulsion system overall length was increased by +15%, as shown in Table 21, resulting in an oxidizer and fuel tank length increase. Other physical dimensions for the motor assembly remained unchanged.

**Mass Properties.** Motor mass (as shown in Table 21) increased because of the +15% stretch.

**Table 21. Comparison of Physical Properties of FIGG and SC HRMs**

<u>Physical dimensions</u>	<u>FIGG</u>	<u>+15% FIGG</u>	<u>SC HRM</u>	<u>+15% SC HRM</u>
Overall propulsion system length, in.	75.0	<b>86*</b>	75.0	<b>86</b>
Outside diameter, in.	7.0	7.0	7.0	7.0
Oxidizer tank length, in.	42.0	<b>49.5</b>	<b>42.9</b>	<b>51.7</b>
Flow control valve length, in.	1.0	1.0	1.0	1.0
Fuel tank length, in.	17.4	<b>19.6</b>	<b>16.5</b>	<b>18.7</b>
Nozzle assembly length, in.	15.6	15.6	15.6	15.6
Nozzle exit diameter, in.	6.0	6.0	6.0	6.0
Nozzle throat diameter, in.	1.9	1.9	1.9	1.9
<u>Mass</u>				
Pressurization system, lbm	2.5	<b>2.8</b>	<b>2.5</b>	<b>2.9</b>
Oxidizer tank, lbm	21.1	<b>24.8</b>	<b>21.6</b>	<b>25.2</b>
Oxidizer outflow valve, lbm	2.4	2.4	2.4	2.4
Injector, lbm	1.0	1.0	<b>1.8</b>	<b>1.9</b>
Injector distribution plate, lbm	0.1	0.1	0.1	0.1
Fuel tank, lbm	10.3	<b>11.4</b>	<b>9.9</b>	<b>11.0</b>
Propellant insulation, lbm	1.6	<b>1.8</b>	<b>1.5</b>	<b>1.8</b>
Nozzle, lbm	7.0	7.0	<b>7.3</b>	<b>7.3</b>
Nozzle insulation, lbm	1.6	1.6	1.6	1.6
Ignition system, lbm	0.4	0.4	0.4	0.4
External insulation, lbm	0.2	0.2	0.2	0.2
Other, lbm	0.6	0.6	0.6	0.6
Total inert weight, lbm	48.9	<b>54.1</b>	<b>49.9</b>	<b>55.4</b>
Oxidizer, lbm	86.9	<b>105.6</b>	<b>89.0</b>	<b>107.4</b>
Fuel, lbm	23.6	<b>28.7</b>	<b>24.2</b>	<b>29.2</b>
Total loaded weight, lbm	159.3	<b>188.4</b>	<b>163.1</b>	<b>192</b>
Mass Fraction	0.69	<b>0.71</b>	<b>0.69</b>	<b>0.71</b>

\*Bold print highlights differences

**Performance.** Increasing the motor length +15%, significantly improved motor impulse. Motor total impulse and burn time increased (shown in Table 22).

**Table 22. Comparison of Performance for FIGG and SC HRMs**

<u>Performance Parameter</u>	<u>FIGG</u>	<u>+15% FIGG</u>	<u>SC</u>	<u>+15% SC</u>
O/F ratio	3.7:1	3.7:1	3.7:1	3.7:1
Chamber pressure, psia	1300	1300	1300	1300
Specific impulse, vac delivered, sec	273	273	273	273
Thrust, vac, lbf	6000	6000	6000	6000
Total impulse, sec	29500	35900*	30200	35500
Burn time, sec	4.9	6.0	5.0	6.1
Nozzle expansion ratio	10:1	10.1	10:1	10:1

Pressurization Requirements

**Solid Propellant**

Propellant density, lbm/in <sup>3</sup>	0.0635	0.0635	0.0635	0.0635
Combustion temperature, °F	2500	2500	2500	2500
Grain outside diameter, in.	6.0	6.0	6.0	6.0
Grain Surface area, in <sup>2</sup>	28.3	28.3	28.3	28.3

**Gas Generator 1**

Burn time, sec	2.9	3.6	3.0	3.7
Required propellant mass, lbm	0.85	1.03	0.87	1.04
Thickness, in.	0.47	0.57	0.48	0.58
Burn rate, in/sec	0.16	0.16	0.16	0.16

**Gas Generator 2**

Burn time, sec	2.0	2.4	2.0	2.4
Required propellant mass, lbm	0.56	0.68	0.58	0.7
Thickness, in.	0.31	0.38	0.32	0.39
Burn rate, in/sec	0.16	0.16	0.16	0.16

\*Bold print highlights differences

**Layout.** The layout for the +15% stretch staged combustion hybrid is shown in Figure 39. The motor assembly is exactly the same as the staged combustion hybrid baseline configuration except for the increased length of selected components.

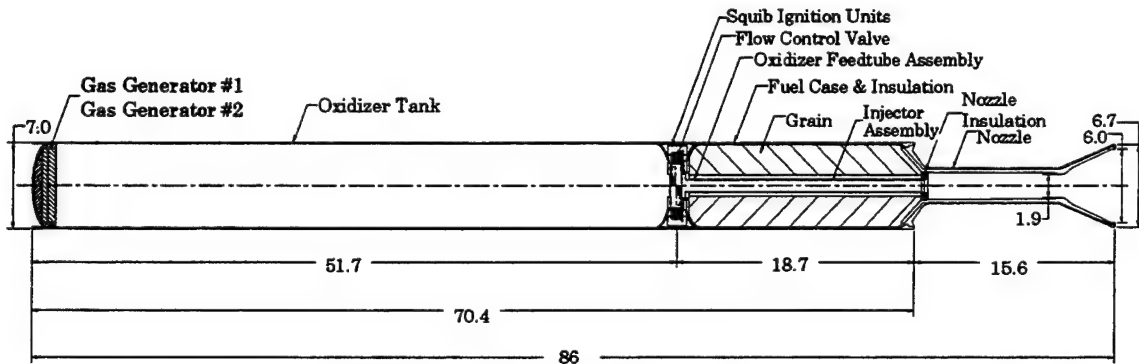


**Figure 39**  
**+15% Length Staged Combustion Hybrid Motor Layout**

**Missile Configuration.** Figure 40 shows all components of the +15% stretch staged combustion hybrid rocket motor integrated into the missile.

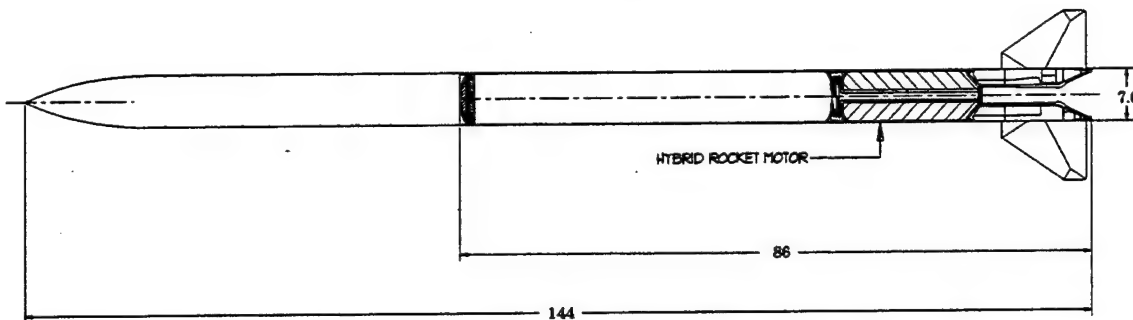


**Figure 40**  
**+15% Length Staged Combustion Hybrid Motor Missile Configuration**

#### 4.4 Engagement Analyses

**4.4.1 Hybrid Motor Performance Characteristics.** Input requirements for the OTIS engagement simulation code include propulsion system thrust, Isp, and usable propellant. Since the engagement flight paths can vary from sea level to high altitude, thrust and Isp versus altitude are necessary for improved fidelity. Four motor/missile systems were selected for analysis: the solid baseline with the standard and +15% motor and the PLOX1/BAMO hybrid with the standard and +15% motor. Using the propellant loads and operating characteristics from the Design Configurations Section (4.3) and the refined performance estimates from the Tactical Missile Hybrid Technology System Study Section (4.2), performance (thrust and Isp) versus altitude were compared. Motor weight statements are consistent with those given in Section 4.3. It was assumed that motor flowrates (thrust and Isp at any given altitude) were constant throughout the burns. Given the high regression rates of BAMO, it should not be difficult to design a neutral (constant burn area) grain. However, detailed grain design was outside the scope of the present study.

**4.4.2 Candidate Missile Flight Performance.** Figure 41 shows the three beyond-visual-range (BVR) air-to-air engagements (the class to which the air-to-air missiles belong) that were used in the performance evaluation. All are "head-on" encounters between a friendly "blue" and an enemy "red" aircraft. These engagements include: a shoot-up encounter against an enemy supersonic interceptor (such as the Mig 25) at higher altitude, a co-altitude encounter against an enemy fighter (such as the Mig 29 or SU-33) at almost the same altitude, and a shoot-down encounter against an enemy "Flogger"-type fighter/bomber approaching ground targets at low altitude to minimize exposure to air defenses.

Figure 41 also shows typical missile range parameters associated with any head-on beyond-visual-range engagement. They include: missile launching range ( $R_L$ ) – the downrange distance of the oncoming red aircraft from the blue aircraft at the instant of blue missile launch; missile intercept range ( $R_i$ ) – the downrange distance traveled by the blue missile between launch and intercept of the red aircraft; and the "f-pole" range ( $R_{fp}$ ) – distance of the oncoming red aircraft from the blue aircraft when red intercept occurs. F-pole range is a very critical parameter because it is indicative of whether the enemy aircraft can be intercepted before launch or lock-on of his missiles against the blue aircraft or against the ground or air targets being defended by blue.

Missile maximum range is the distance beyond which the missile has insufficient flight speed to accomplish needed end-game maneuverability to cope with evasive maneuvers by the enemy aircraft during the final phase of missile flight. A rule of thumb for estimating required end-game maneuverability (for nulling guidance errors and coping with target evasive maneuvers) is that the missile should be capable of 2 to 2.5 times the maneuverability of the enemy aircraft when

its evasive maneuver begins. Thus the intercept criteria selected for this analysis was that the missile should possess sufficient intercept speed to generate 2.5 times target acceleration at maximum missile angle of attack which, for tail-controlled beyond-visual-range missiles (BVRMs), is approximately 20 degrees.

The OTIS trajectory optimization program was used to optimize each BVRM trajectory to maximize the f-pole range of each BVRM for each of the three engagements. Constraints include end-game maneuverability requirements, axial and lateral g-limits, missile angle of attack, and maximum flight times. The optimization program also determined the interval between the two major burns of the hybrid rocket motors for maximum f-pole trajectory.

Previous air-to-air studies have shown that missile propulsive energy can be more effectively expended in two major burns, rather than only one, with approximately 60% of motor impulse expended in the first burn and the delay between burns determined by the type of engagement and required intercept range. Varying thrust within a burn is not particularly useful and results in the lowering of Isp. Thus it was assumed that the hybrid rocket motors would deliver their impulse in two full thrust burns. Figure 42 shows the thrust and impulse characteristics selected for the two burns with the missile flight profile associated with the delay of the second burn. In general, a third burn was found to provide only a slight improvement beyond what was possible with two burns.

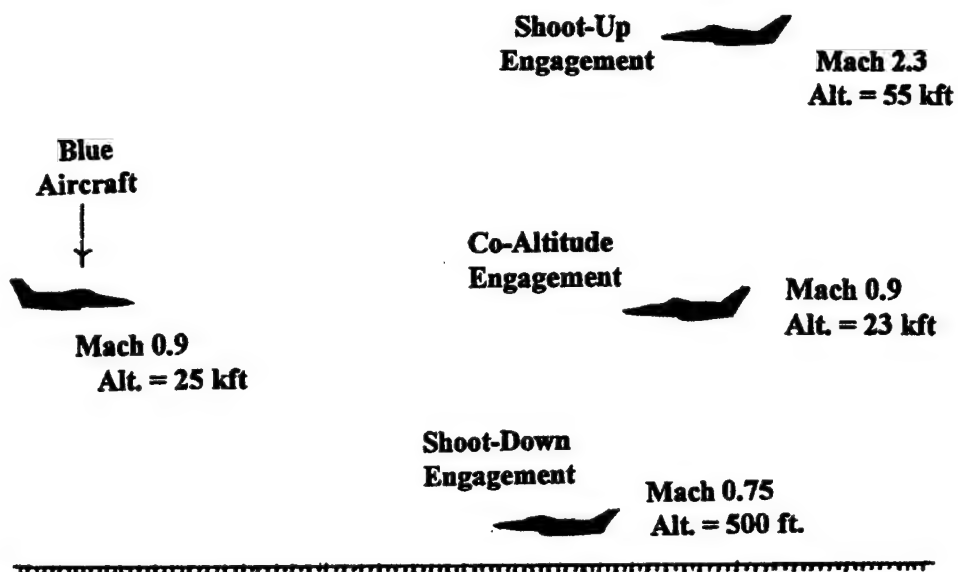
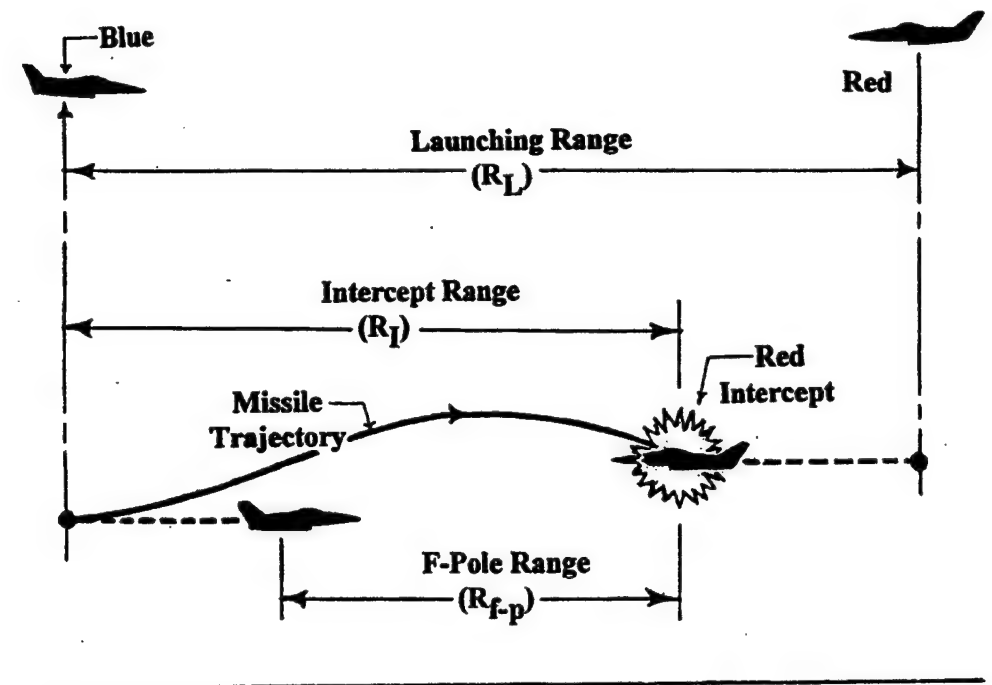


**Figure 41**  
Engagement Geometries and Selected Engagements

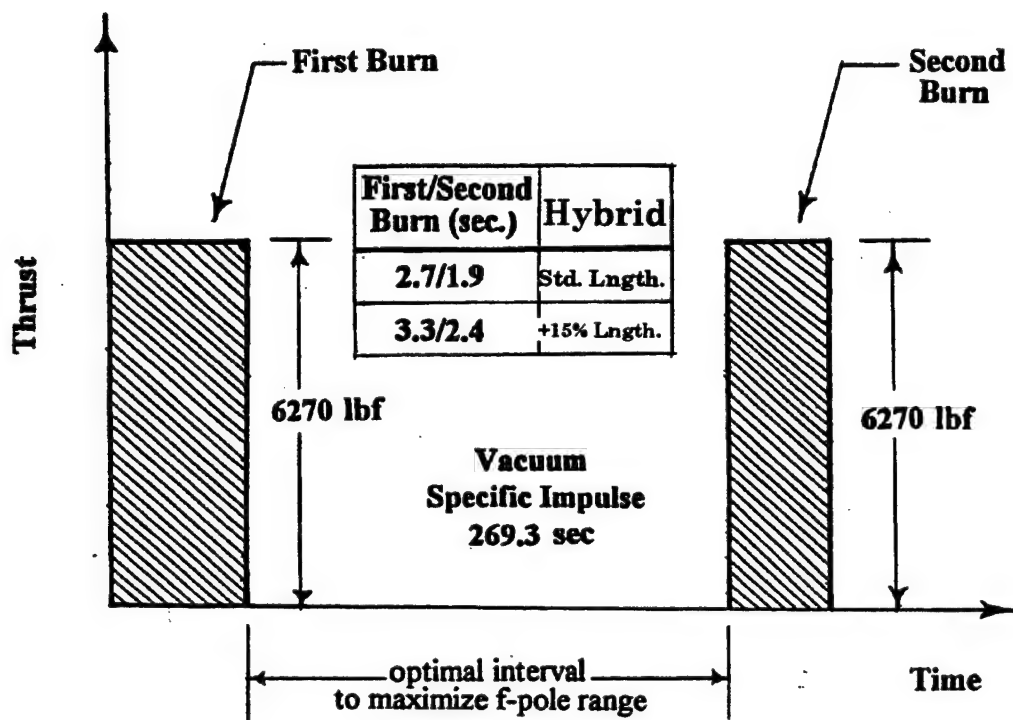
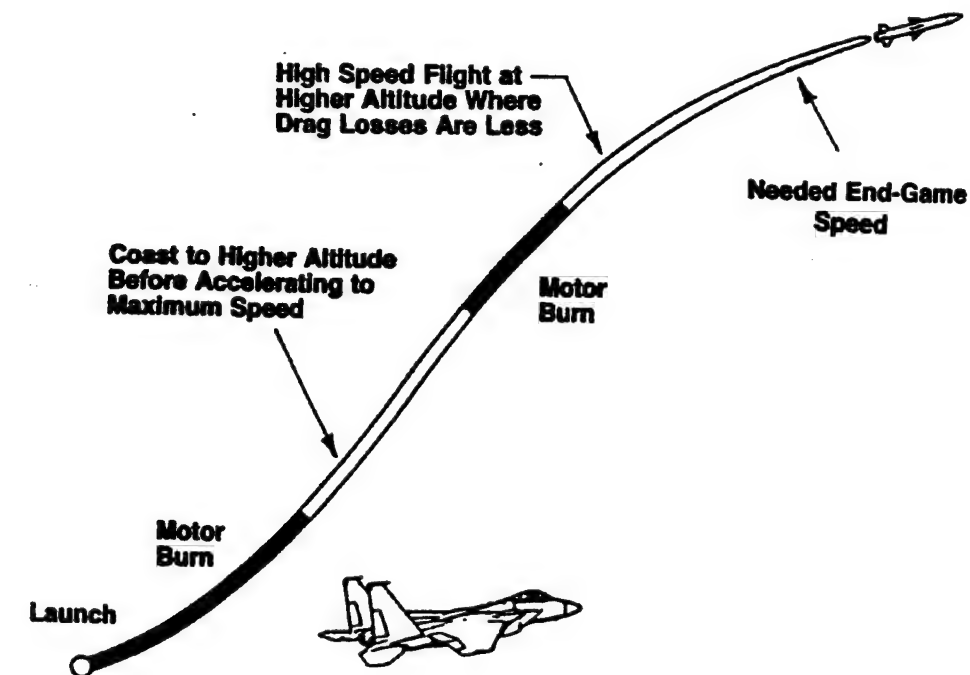


**Figure 42**  
**Trajectory Shaping and Propulsive Energy Management**

Missile and trajectories were constrained by lateral and axial accelerations typical of BVRM structures and components, BVRM angle-of-attack capability, and terminal maneuverability requirements. Figure 43 shows the missile flight constraints associated with each of the three engagements.

Initial missile performance evaluations limited BVRM maximum flight time to 125 sec (about 50% longer than current BVRM power systems allow). Later evaluations removed all missile time-of-flight limits to estimate maximum BVRM performance. However, these evaluations retained a 400 psf minimum dynamic pressure limit, which is necessary for missile maneuvering. This limit will determine maximum altitude ceiling.

"Staged combustion" hybrid rocket motors with the PLOX1/BAMO propellant combination were used in the engagement analysis. An impulse split of 58% and 42% was used for the first and second burns. These burns are separated by a delay time that can be zero or significant, depending on the optimum mission engagement.

Axial force coefficient (CA) characteristics were estimated for the thrusting (power-on) phases of missile flight and for the coasting (power-off) flight phases. Without power, drag is greater because less pressure acts on the missile base in the absence of the rocket exhaust. Aerodynamic characteristics were initially computed using the Air Force DATCOM aerodynamic prediction code. However, this program appears to underpredict both normal force coefficient (CN) and CA at higher angles of attack. Therefore, modified BVRM aerodynamic characteristics formulated by Integrated Systems Incorporated (ISI) were used.

Nonpropulsive missile weights were based on generic air-to-air BVRM weight statements. The kinematic performance parameters for each BVRM include missile powered flight and coasting time, maximum flight altitude, and speed, as well as missile intercept time, maximum f-pole, intercept, and launching range for each engagement.

Type of Engagement	Axial Acceleration g Limit	Lateral Acceleration g Limit	Angle of Attack Limit	Minimum Lateral Acceleration @ Intercept
Shoot-Up	30	30	20 deg.	6.0g
Co-Altitude	30	30	20 deg.	17.5g
Shoot-Down	30	30	20 deg.	12.0g

**Figure 43**  
**Flight Constraints and Missile Configurations**

**4.4.3 Engagement Analysis Summary.** Previous pulse motor studies indicated that separated full thrust burns are preferable and that the added complexity of throttling is not needed for air-to-air missile engagements. This study confirmed the usefulness of separated constant thrust burns for very long air-to-air intercept ranges.

Hybrid rocket motors that can deliver more impulse and impart more missile speed than solid rocket motors enable higher altitude flight. This results in less velocity slowdown because of lower drag and enables longer BVRM flight times and higher average speed. The longer flight times and higher average flight speeds provide much greater f-pole, and intercept and launch ranges.



#### **4.5 Tactical System Summary**

From the design analyses, it was established that the total impulse of the hybrid systems was greater than their solid counterparts, even though the hybrid systems' mass fractions were slightly lower. Within the fidelity of the study, the FIGG cycle and the staged combustion mass fractions were similar (2 to 3% difference). However, critical hybrid technologies for achieving high hybrid mass fractions will be the oxidizer pressurization and expulsion system, and lightweight, compact multiple-use oxidizer control valves.

The engagement analyses showed that energy management can yield improvements in flight performance. It was found that motor throttling was unnecessary and that two full-thrust burns could achieve most of the potential gains. The missiles are operating in a nonlinear regime where small gains in velocity (from greater impulse) are magnified because of the ability to fly higher where drag losses are reduced. F-pole ranges for the hybrids were characteristically greater than the solids.

## **5.0 TACTICAL TECHNOLOGY DEVELOPMENT ELEMENTS**

Many hybrid tactical propulsion system areas are unproven and require development. Where possible, the ideas and concepts selected for this study were derivatives from previous and current programs sponsored by various government agencies (e.g., PL, NASA, BMDO, etc.). However, in establishing development programs, consideration should be made to technologies which have multiple cycle application or that are critical to the implementation of a cycle.

### **5.1 Cycle Common Elements**

Both the classical and the staged combustion hybrid rocket motors have a family of "cycle common" items which are required for successful operation. These are:

- Oxidizer tank and expulsion system
- Pressurization system
- Flow control valve
- Motor case
- Propellant insulation
- Nozzle
- Nozzle insulation
- Squib ignition unit

Although these are common to each design, it is important to note that detailed trades will yield variations in the implementation of each component.

### **5.2 Cycle Unique Elements**

Within each design there are several items that are unique to their cycle. These are:

#### **Classical Hybrid**

- Injector/distribution plate
- Solid propellant (less so with the FIGG cycle variation)

#### **Staged Combustion Hybrid:**

- Injector/feed tube/distribution plate
- Solid propellant

## **6.0 SUMMARY AND CONCLUSIONS**

This study has found that hybrid propulsion is a viable prospect for improving propulsion technology in tactical missiles. The niche for hybrid propulsion in the tactical area primarily lies in applications that require insensitive munitions and improved energy management over current applications. This study recommends that the Air Force should develop hybrid technology based on the fuel-rich, solid gas generator concept. The tactical mission will have the option to pursue forward- or aft-injected technologies.